

Precision wavelength calibration for Radial Velocity measurements using Uranium lines between 3800-6900 Å

Rishikesh Sharma^{a,*}, Abhijit Chakraborty^a

^aAstronomy & Astrophysics Division, Physical Research Laboratory, Ahmedabad 380009, India

Abstract. We present here the precise wavelength calibration of a high-resolution spectrum using Uranium (U) lines in the wavelength range of 3809 - 6833 Å for precision radial velocity measurements for exoplanet detection or related astrophysical sciences. We identify 1540 well-resolved U lines from a high-resolution ($R=67,000$) spectrum of the uranium-argon hollow cathode lamp (UAr HCL) using PARAS spectrograph in the aforesaid wavelength range. We calculate the neutral and first allowed transitions (Ritz wavelength) of U from its known energy levels and compare them with our observed central wavelengths. We measure an offset of -0.15 mÅ in our final U line list. The line list has an average measurement uncertainty of 15 m s⁻¹ (0.013 pixels or 0.28 mÅ). We included these lines to the PARAS data analysis framework to perform the wavelength calibration and then calculate the multi-order Radial Velocity (RV) of PARAS spectra. The typical dispersion of residuals around the wavelength solution of a UAr spectrum, using U lines, is found to be 0.8 mÅ (~ 45 m s⁻¹). With the use of this line list, we present our results for the precision RV of an on-sky source (A RV standard star), and an off-sky source (A HCL) observed with PARAS along with UAr HCL. We measure the dispersion in absolute drift difference between two fibers (inter-fiber drift) for a span of 6.5 hours to be 88 cm s⁻¹, and the RV dispersion (σ_{RV}) for a RV standard star, HD55575 over the course of ~ 450 days to be 3.2 m s⁻¹. These results are in good agreement with the previous ones measured using the ThAr HCL. It proves that the ThAr HCL with $\sim 99\%$ pure-Th are replaceable with the UAr HCL for the wavelength calibration of the high-resolution spectrographs such as PARAS ($R \leq 67,000$) to achieve a RV precision of $1-3$ m s⁻¹ in the visible region.

Keywords: hollow cathode lamps, wavelength calibration, high-resolution spectrographs, radial velocity.

*Rishikesh Sharma, rishikesh@prl.res.in

1 Introduction

The sudden increase in the population of exoplanet candidates in the last decades from various space-based (like CoRoT,¹ Kepler & K2,² TESS,³ etc.) and ground-based transit surveys (like SuperWASP,⁴ KELT,⁵ etc.) has opened a quest among the scientific community to build the high-precision radial velocity (RV) spectrographs, which can go down to sub - 1 m s⁻¹ of RV precision and eventually, detect and confirm the exoplanet candidates. One of the main challenging aspects for such instruments is the wavelength calibration technique, which is evolved from the initial and established techniques of iodine cell and hollow cathode lamps (HCLs) to Fabry-Perot etalon and highly precise high-frequency laser combs. The laser frequency combs (LFCs) used in various spectrographs like EXPRES⁶ ESPRESSO,⁷ HARPS,⁸ HPF,⁹ etc., are the latest and most precise equipment for the wavelength calibration that have shown upto 2.5 cm s⁻¹ of RV precision on HARPS⁸ over a short-term (2 hours).¹⁰ Besides being the most advance system for wavelength calibration, the use of LFCs is limited due to their cost and complexity. Alternatively, the conventional system for calibration, like HCLs¹¹ (e.g., ThAr), is widely used in the astronomical spectrographs due to their relatively long life, easy handling, simple structure, and less maintenance. Th metal being a single isotope, having narrow lines and a dense spectrum, is used for the wavelength calibration of the astronomical spectrographs. PARAS (PRL Advanced Radial-velocity Abu-sky Search)^{12,13} is a precision radial velocity fiber-fed, temperature and pressure-controlled spectrograph connected to a 1.2m telescope at PRL Mt. Abu Observatory in Gurushikar, Mt. Abu, India.

The high-precision RV spectrographs like HARPS and PARAS have used Th-Ar HCL for wavelength calibrations and shown long-term stability up to 0.8 m s^{-1} ¹⁴ and 1 m s^{-1} ,¹² respectively. The long-term stability here refers to the RV stability achieved over the course of 3 months or more.

The ThAr HCLs from S & J Juniper & Co¹ are currently used in many precision Radial-Velocity spectrographs. However, these HCLs with a cathode made of pure Th (up to 99% purity) are no more commercially available; instead they are available with a cathode made of Thorium-Oxide (ThO). 15 confirmed that this oxide impurity is responsible for the presence of molecular oxide bands and other unwanted features in the HCL's spectra. Thus, it becomes difficult to identify the faint Th atomic lines in the oxide bands and make them useless for wavelength calibration in some regions, making it tough to precisely characterize and track the Th lines. It degrades the precision of wavelength calibration of high-resolution spectra and, ultimately the RV precision. It becomes paramount to choose the proper element, which can replace the Th element in the HCLs and equally have a vast number of transitions to provide precise wavelength calibration for the astronomical spectrographs.

We looked into the actinide series of the periodic table and found that U fits closest to the Th, and U HCLs are also readily available in the commercial market. The U HCLs are available with cathode made of natural U. Unlike Th, the U atom is found in three isotopic forms in nature namely U^{238} , U^{235} , and U^{234} , with abundances of $\sim 99.275\%$, $\sim 0.720\%$, and $\sim 0.005\%$, respectively. 16 showed that the second most abundant isotope has a hyper-fine structure, and thus its features spread over many lines with very less intensity and won't cause any significant problem in RV precision. Even, the recent study by 17 (Here on, S18) showed that the U could replace the Th in ThAr and Thorium-Neon (Th-Ne) HCLs for the wavelength calibration in the visible and NIR range more precisely as U has more number of lines than Th in both the wavelength regions. However, their line list starts from mid-visible and stretches up to NIR, i.e., in the wavelength range of 5000-17000 Å, which does not fully cover the PARAS wavelength range of 3809-6833 Å. 18 (here on, P80) was also previously published the U line list in the wavelength range of 3846-9091 Å. We acknowledge both previous works of P80 and S18. The P80 line list covers the whole range, which is used for the wavelength calibration in PARAS spectra and hence, more suitable for comparison with our line list. Despite having more lines than Th in the visible range, U lines have never been checked a priori for long-term stability with high-resolution spectrographs.

This work is primarily focuses on the precise wavelength calibration of an astronomical spectrograph like PARAS using the U lines in the visible band (3809 Å - 6833 Å) for radial velocity precision of $1\text{-}3 \text{ m s}^{-1}$ for exoplanet detection, characterization and, related astrophysical sciences. Here, we measure the radial velocities of a well-known RV standard star HD 55575 over a period of 450 days in order to check the feasibility of using U lines instead of Th lines for precision RV measurements of stars.

We describe the observations with PARAS in section 2, while section 3 focuses on the data reduction and wavelength calibration of the UAr spectrum for identifying the lines. Section 4 elaborates the algorithms used for identifying the line features from a UAr spectrum and various steps involved in selecting the final line list, including those from U I and U II transitions. In section 5, we compare the observed central wavelength of selected lines and the calculated Ritz wavelength and discuss the final line list. In section 6, we incorporate the U line list in the PARAS wave-

¹<http://www.sjjuniper.com>

length calibration framework to do the RV measurements on a RV standard star HD55575 and show the on-sky performance for 450 days for the long-term stability of more than a year. Section 7 describes the possible future works, while section 8 summarizes our results.

2 PARAS Observations with UAr HCL

2.1 Experimental set-up

We acquired the high-resolution spectra of the UAr HCL using the PARAS spectrograph¹² coupled with the 1.2m telescope at Gurushikhar Observatory, Mt Abu, India. The UAr HCL from PHOTRAN PTY LTD. is used for the experiment. The spectrograph works at a resolving power of ~ 67000 at the blaze peak wavelength of 5500 \AA . It is a white-pupil configuration fiber-fed spectrograph kept inside a thermally controlled vacuum chamber. There are two fibers, namely star-fiber (or A fiber) and calibration-fiber (or B fiber) that feed the starlight and calibration lamp light into the spectrograph, respectively. Inside the vacuum chamber, the light beam from both the fibers is collimated by an off-axis parabolic mirror, then dispersed by an R4 echelle grating, and then cross-dispersed by a prism, re-imaged onto the $4k \times 4k$ e2v CCD, which has a pixel size of $15 \mu\text{m}$. The details of the spectrograph are given in 12. The CCD detector has a sampling of ~ 4 pixels and an average dispersion of 0.021 \AA per pixel. It implies that each pixel corresponds to a velocity of 1145 m s^{-1} . The previous study by 11 has represented that a HCL's life and intensity of the emitted lines are strongly dependent on the operating current (OC). The increase in OC increases the line intensities and number of transitions but reduces the HCL's life. We set the OC to 10 mA to have a sufficient number of U transitions and, at the same time, to increase the HCL's life. We use the C610 HCL power supply from Cathodeon², which provides the current stability up to 0.05% after the warm-up time of 15 min, throughout the observations. We note here that the HCL was kept switched on throughout the night of observation.

2.2 Off-sky Observations

Initially, we acquired a spectrum of the UAr HCL by illuminating its light in the star-fiber (or A-fiber) to identify the U emission lines. In order to do the initial wavelength calibration of the acquired UAr spectrum, a ThAr spectrum was also acquired in the same way just before the UAr spectrum. The spectrograph stability is such that the drift between the ThAr and the UAr spectrum is negligible for our purpose. We did not use a neutral density filter for off-sky observations, and set the exposure time at 400 sec to have the high SNR spectra as well as to make sure that the high-intensity lines should not saturate the CCD.

We also acquired a series of 400s UAr exposures by simultaneously illuminating the UAr HCL's light in both the fibers (A and B fibers) for ~ 6.5 hours, to track each line's stability and calculate the instrumental drifts for the mentioned time interval.

2.3 On-sky Observations

We observed a RV standard star HD55575, for the span of 450 days, acquiring 27 spectra during the period. These observations were done by illuminating the A-fiber with the starlight and simultaneously illuminating the B-fiber with the UAr light for precise wavelength calibration. The

²https://www.msscientific.de/hollow_cathode_lamp_power_supply.htm

exposure time for these observations was set to 1200 sec, and the SNR ranges between 70-80 at 5500Å. We use the neutral density filter (FSQ-OD50 from Newport)³ with the UAr HCL for these long exposures to ensure that the high-intensity lines should not saturate the CCD. These spectra are used to calculate the RV precision achievable on stars with UAr HCLs (see Sec 4).

3 Data Reduction and Analysis

We used the custom-designed automated pipeline¹² to extract the U spectra from PARAS 2-D (2 dimensional) images. The pipeline is based on the REDUCE package of the 19, which is an optimal extraction code to extract the cross-dispersed echelle spectra. We use the existing ThAr wavelength calibration process to do the initial wavelength calibration of the UAr spectrum, as described in 12. The ThAr spectrum, which was acquired just before the UAr spectrum as discussed in sec 1, is wavelength calibrated using this existing process in the PARAS pipeline. The pipeline uses a template of Th lines for the wavelength calibration. A template is defined here as an order-wise list of central wavelengths of Th lines to use for wavelength calibration. The template has a total of around 1000 Th lines with at least 8 lines per order. For a particular order in the ThAr spectrum, the pixel position of the central wavelength for each line is found, and then a Gaussian is fitted to precisely determine the line position in terms of pixels. These fitted pixel positions and the line's central wavelengths for that order are then fit with a third-order polynomial. The resultant polynomial is used as the wavelength solution for that order. In this way, the wavelength calibration is done for all the 70 orders. This ThAr wavelength solution is applied over the UAr spectrum which was acquired for the line identification process.

4 Identification and selection of U lines

The wavelength calibrated UAr spectrum is now used for the line identification and selection process. The echelle spectra have overlapping wavelength regions over the two consecutive orders. We stitched the UAr spectrum distributed among various echelle orders for line identification and characterization by weighing the overlapping regions in the two consecutive orders according to their S/N ratio. This stitched spectrum is further used for the line identification process.

First, we identified all the line features present in the stitched UAr spectra, based on the slope of the spectra at each point, considering only those features with S/N ratio ≥ 30 , to minimize the uncertainties in finding the central wavelength ($\sigma_\lambda < 1 m\text{\AA}$). We characterized each of these identified lines by fitting them with the MPFITPEAK²⁰ Gaussian function, written in IDL, and determined the line parameters. We have identified nearly 4500 emission features in this step. The intensities of these lines spread across the whole dynamic range of the CCD detector, and 3 high-intensity lines among them falling at 5915.3867, 6449.1625 & 6826.9185 Å, are found to be saturated. These lines are not considered for further selection and are excluded from the identified lines.

The lines identified in the last step are supposed to be emitted by either cathode filling metal U or the filling gas Ar. It is well-known that the Ar lines are not suitable for the precise wavelength calibration and can show wavelength drifts of tens of m s⁻¹.²¹ The next step in the U line selection procedure is to remove the Ar lines. So, we identified the Argon lines using the 21 ThAr line list, based on the fitted central wavelength of each line's Gaussian profile and eliminated them for the

³<https://www.newport.com/p/FSQ-OD50#mz-expanded-view-462354496971>

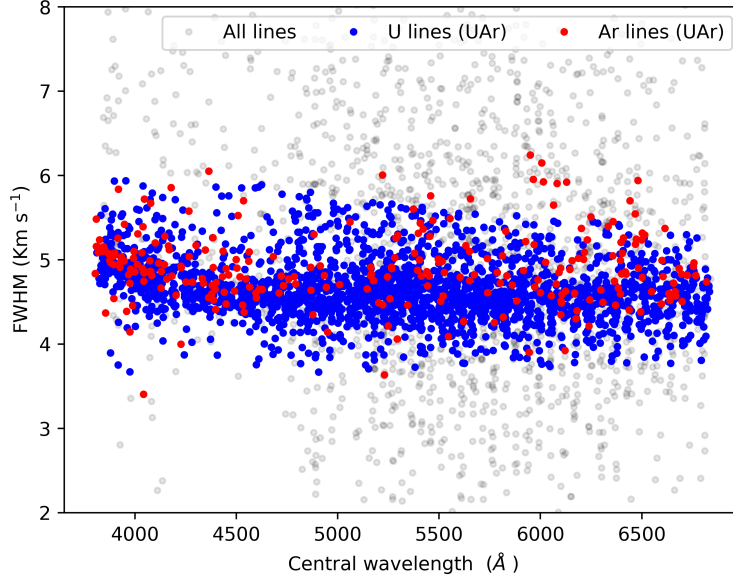


Fig 1: The FWHM of all the 4500 emission features identified in the first step (see Sec 4) is plotted here in grey color. Overplotted in red are the widths of 270 Ar lines identified in Sec 4. The blue dots represent the line widths of the 1819 lines of the preliminary U line list (see Sec 4). It can be seen that the selected U lines and identified Ar lines are consistent with the instrumental resolution and have line widths between $3.75 - 6.0 \text{ Km s}^{-1}$.

further selection process. 21 used the HARPS spectrograph for their work. Since HARPS has a higher resolution than PARAS, all the Argon lines from our spectra must be listed in the cited line list. We could identify 270 Ar lines in the UAr spectrum and removed them from the lines identified in the last step. We have plotted the line widths (FWHM of the Gaussian) of Ar lines in red color in Fig 1. It can be seen that their line widths are consistent with the PARAS instrumental resolution. The blended lines present in the UAr spectra can induce the centroid shifts much larger than the measurement errors associated with line positions. Therefore, It is better to remove the possible blends from the remaining lines. We used the line width of the remaining lines to identify the blends. Since the instrument works at a certain resolution ($R \sim 67,000$; 4.5 Km s^{-1}), we only considered those lines whose widths are consistent with the instrumental resolution and lies within $3.75 - 6.0 \text{ Km s}^{-1}$. This eliminates the possible dangerous blends in the UAr spectra to be included in our further selection of the lines. In fig 1, we have plotted the line widths of all the identified lines in grey color. The lines which pass the above selection criteria have been highlighted in blue. In fig 1, few lines among 4500 lines with significantly smaller line widths ($\leq 3.75 \text{ Km s}^{-1}$) can be seen, which could be due to some artifacts or bad pixels and hot pixels in the CCD detector. As a precaution, we also removed those lines which appear single in our spectra but have other line features within, listed in the P80 line list, due to a much higher resolution of the instrument used by them ($R = 600,000$).

Since our main aim is to do the precise wavelength calibration of the spectrograph using UAr spectra, we strictly consider the lines that are well resolved or well-separated from their neighbors to fit a single-peaked 1-D (1-dimensional) Gaussian. This implies that the two neighboring lines

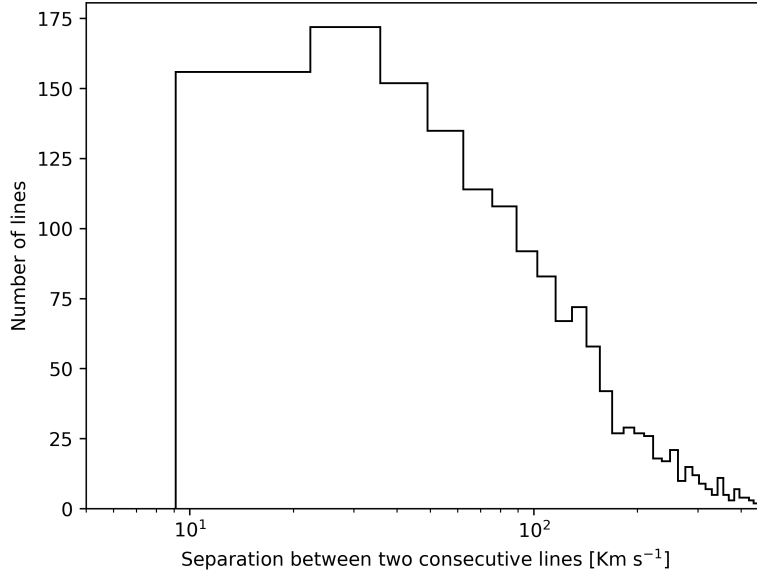


Fig 2: The histogram plotted here shows the separation in Km s^{-1} between two consecutive lines from our final line list. The minimum separation is $\sim 9.0 \text{ Km s}^{-1}$, which is nearly the two resolution element PARAS, and shows that the lines in our line list are well-separated. The x-axis is in the log scale.

with least separation of 2-resolution elements are considered for further selection. We have plotted a histogram (see fig-2), which shows the distance between two consecutive lines from the final line list. The minimum separation between two lines is 9.0 km s^{-1} , which nearly equal to 2-resolution elements of PARAS.

In this way, the total number of lines selected after passing through each of the above selection steps was 1819. We call this line list as the preliminary U line list. The instrumental resolution calculated using these lines by measuring their line widths is plotted in fig-3. The median resolution of the spectrograph is 67000.

5 The Final U line list

The preliminary line list possibly contains the lines which are not exactly the U transitions or for which energy levels are unknown. It is also possible that the UAr spectra may contain more Ar lines than the ThAr spectra, which are mentioned in 21 (see sec 4). As stated before, we do not want to include any Ar line in the final line list; therefore, we compared all the lines from the preliminary line list with the possible theoretical transitions. We calculated the Ritz wavelength using the energy levels for the first and the second transition of U found at actinides database ⁴, considering the selection rule for possible allowed electronic transitions.²² With the known energy levels, there are 96936 possible transitions in the wavelength range of 3809-6833 Å. We calculated the difference between all our lines and the closest line from the theoretical line list, and plotted its distribution in Fig 4. The median of the distribution is found to be -0.15 mÅ , with a standard deviation (σ) of 2.1 mÅ . The standard error of median is 0.061 mÅ , which shows that the offset

⁴<http://www.lac.u-psud.fr/old-lac/lac/Database/Tab-energy/Uranium/>

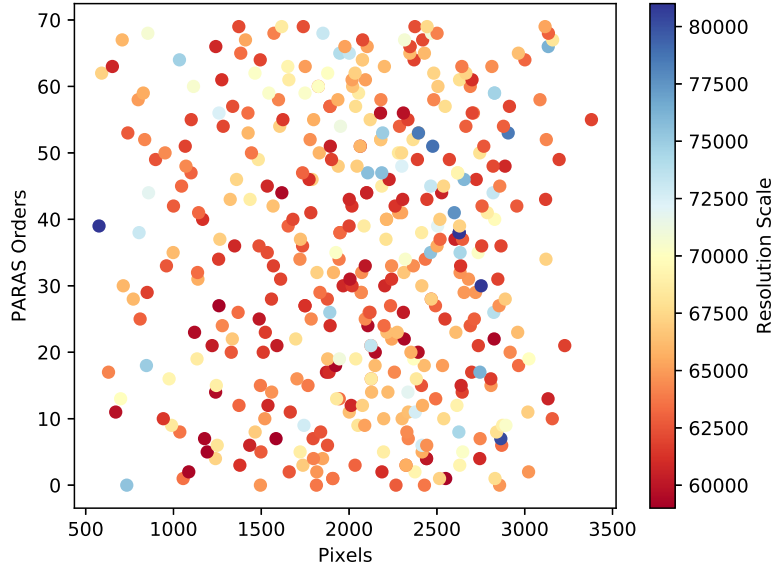


Fig 3: The resolution of acquired UAr spectrum in various orders. It can be seen that the spectral resolution is in the range of 60000-80000. The color coding here represents the resolution and, the median resolution is 67000.

is considerable. The observed lines that lie within the 3σ of the median of this distribution from their closest Ritz wavelength are selected for the final line list. The final line list contains a total of 1540 U lines. The remaining 279 lines from preliminary line list are either U lines for unidentified energy levels or atomic lines for other elements that may be present as contamination in U. The identification of these lines is not in the scope of this paper, and we simply rejected these lines.

The finally selected lines are listed in Table-1, which has 7 columns. The uncertainties reported in the table are the errors associated with each line while determining the line position, computed from the covariance matrix using the MPFITPEAK²⁰ Gaussian function written in IDL. The major contributor in these errors is the photon shot noise corresponding to the line intensities and they range between 0.02 - 0.9 mÅ. The final line list has an average measurement uncertainty of 15 m s⁻¹ (0.013 pixels or 0.28 mÅ). The strongest line has a measurement uncertainty of ~ 1.2 m s⁻¹ (0.001 pixels or 0.02 mÅ), while the faintest line has been measured with a precision of ~ 50 m s⁻¹ (0.043 pixels or 0.9 mÅ). It is also observed that the median photon noise errors of the lines falling at the edges are 14 % higher than the lines falling at the center of the CCD. This is because that lines falling on the edges of the detector, where orders are stitched together may have slight asymmetric point spread function (PSF), which leads to higher errors. The various distributions of uncertainties are plotted in fig 5. It is to note here that the Th lines used for initial wavelength calibration of the U lines has a median offset of ~ -1.5 mÅ from the absolute wavelength scale of the 21 line list, and that offset has been corrected before comparing the U lines (from preliminary U line list) with Ritz wavelengths.

We have also compared our final line list with the P80 line list. The P80 line list is the only previously published line list which covers the whole wavelength range used in our work. They

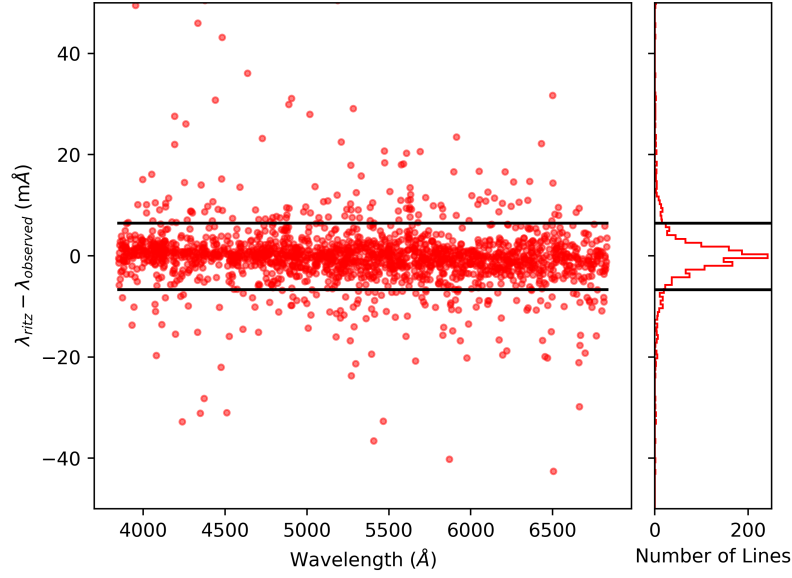


Fig 4: The distribution of differences between observed central wavelengths in this work and the Ritz wavelength. The left panel is the scatter plot of the distribution. The median and standard deviation (1σ) of the distribution are -0.15 and 2.1 mÅ, respectively. The right panel is the histogram of the same data. The two black lines represent the $\pm 3\sigma$ limits of the distribution.

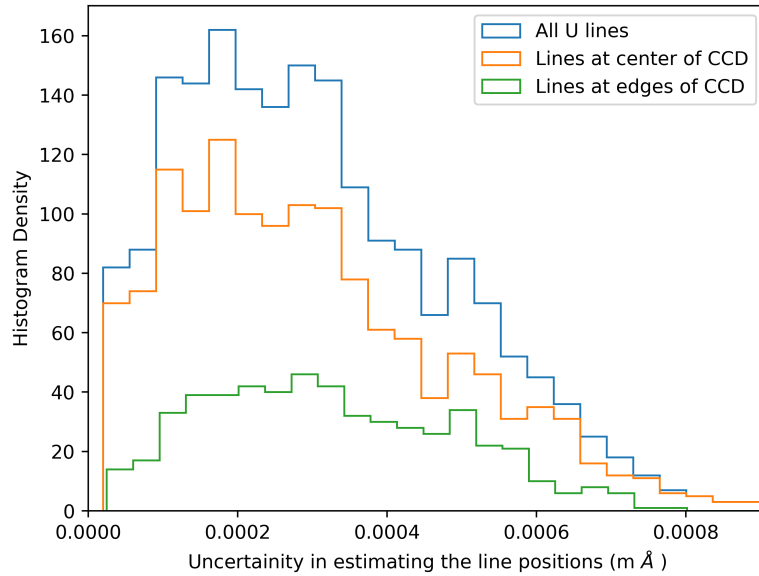


Fig 5: The histogram plot for the uncertainties with which we find the positions of each line in the final line list in mÅ, is plotted in blue. The mean error is 0.28 mÅ. The orange and green colored histograms show the error distributions of the lines falling at the central part of the CCD and the edges of the CCD with a mean of 0.27 mÅ, and 0.31 mÅ, respectively.

used Fourier Transform Spectrograph (FTS) for the line identification work, and reported around 3700 lines in the PARAS wavelength range. We found that $\sim 90\%$ of the lines in the final line list are from P80, and the remaining are newly identified in this work. These newly identified lines are flagged as 'RS21' in the line list, while the remaining have been flagged as 'P80' (see Table-1). In the 1980s, Photo Multiplier Tubes (PMTs) were generally used as detectors, while we use a CCD as a detector, which has much better quantum efficiency than the former. It results in better sensitivity and thus, we could detect the fainter lines missed in P80 work. Also, new energy levels have been identified after the P80 work, found at the actinides energy database, are included in this work^{5,6}. The number of lines in our line list is less than the P80 line list as our resolution is much lesser than the FTS ($R = 600,000$), and our line list only contains the lines, which are clearly resolved and their line positions are precisely determined. Besides that, we have found that there is no significant offset in the absolute wavelength scale in our line list from P80 line list. The main advantage of our line list is that the photon noise uncertainties in determining the line positions are much lesser than the P80. The P80 line list determined the line positions with an average precision of $2 \text{ m}\text{\AA}$, while the median error of our line list is $0.28 \text{ m}\text{\AA}$, which is ~ 7 times better than the P80 line list errors.

6 Results and Discussions

6.1 Performance of the instrument using UAr HCL

We measured and found that the fundamental precision achievable with the UAr spectra is 20 cm s^{-1} , while it is 18 cm s^{-1} with the ThAr spectra in PARAS, calculated using the algorithm explained in 23. To check the stability of the UAr HCL with the instrument and to track the instrumental drift, a series of continuous UAr-UAr exposures is acquired for ~ 6.5 hours as described in section 2. A template of the U lines from the final line list is used for the wavelength calibration of these spectra. The template is created in the same manner as described in section 3. This template is replaced with the previously used Th lines template in the PARAS data analysis framework, and the wavelength calibration of the spectra is done using the same methodology as described in section 3. For an order, the new pixel position of each line belonging to that particular order is estimated and, then a third-order polynomial is fitted over these new positions and the central wavelength of the lines in the template. Then that polynomial solution is applied over the whole order. The same procedure has been iterated for all the 70 orders. In this way, the wavelength calibration of all the UAr-UAr spectra was done. The instrumental drift is calculated by cross-correlating each of these UAr spectra with a binary mask of U lines used in the wavelength calibration. The binary mask is defined as a template spectrum of U, which consists of several box-shaped or rectangular functions, each of them centered at U line position and has a constant value over the width associated with that line and is zero elsewhere. We have plotted the instrumental in fig 6. The upper panel shows the absolute drift in both the fibers, while the lower panel depicts the relative drift between the two fibers with respect to time. Since both the fibers (fiber A & fiber B) pass through the same opto-mechanical elements and see same minute changes in pressure and temperature, therefore the drift in each fiber should be identical.¹² We find that both the fibers drift identically (see fig 6, upper panel) and the 1σ scatter in the absolute drift is ~ 75

⁵<http://www.lac.u-psud.fr/old-lac/lac/Database/Tab-energy/Uranium/U1-ref.html>

⁶<http://www.lac.u-psud.fr/old-lac/lac/Database/Tab-energy/Uranium/U2-ref.html>

m s^{-1} in fiber A as well as in fiber B. However, there is a better way to represent the achievable RV precision of the spectrograph using the differential drift (or inter-fiber drift) between both the fibers.¹² In PARAS, we use the simultaneously acquired calibration lamp's spectrum for the wavelength calibration of a stellar spectrum in order to correct the absolute instrumental drifts. Also, the inter-fiber drift is corrected using the UAr-UAr exposures acquired just before and after the stellar spectrum and that minimizes the wavelength calibration errors. Therefore, the 1σ scatter of this inter-fiber drift exhibits the RV precision due to the wavelength calibration errors. Here, the 1σ of the differential drift ($\sigma_{\text{driftA}-\text{driftB}}$) is found to be 0.88 m s^{-1} . Earlier, with the ThAr HCL, this 1σ scatter was 0.92 m s^{-1} .¹² These results are comparable as the 1σ scatter of the differential drift from both the HCLs is in good agreement with each other. It is to note here that the typical dispersion in the differential drift with a UAr HCL on a night is $\leq 1 \text{ m s}^{-1}$, and it also represents the wavelength calibration precision. This demonstrates that the UAr HCLs can replace the ThAr HCLs in PARAS-like spectrographs for achieving the wavelength calibration precision up to 1 m s^{-1} . PARAS-like spectrographs here refer to the spectrographs with similar spectral resolution ($R \leq 70,000$) as PARAS, similar pressure and temperature stability as described in 12 and uses the similar calibration system (like ThAr or UAr HCL).

Furthermore, we checked the residuals around the wavelength solution of a UAr spectrum from

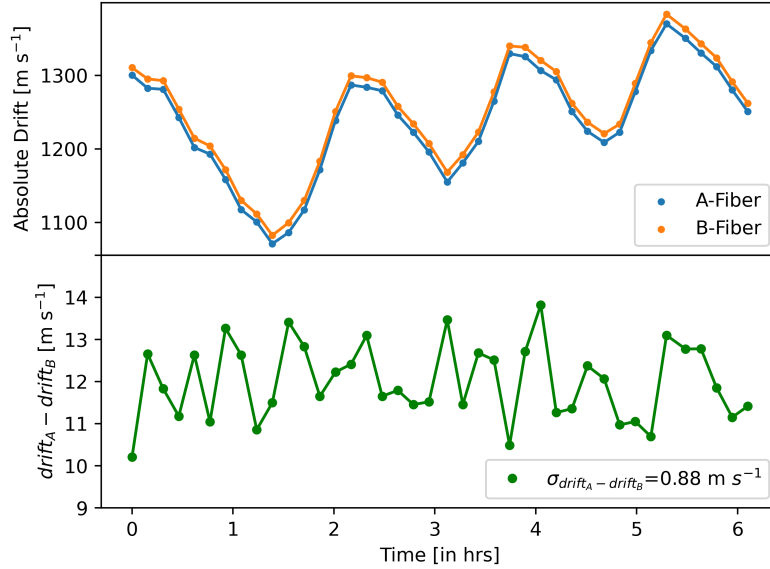


Fig 6: Upper Panel:- The figure shows the absolute drift in A and B fiber with respect to time. The dispersion in absolute drift is 75 m s^{-1} in both fibers. It can be seen that both the fibers track each other very well. Lower Panel:-The figure shows the inter-fiber drift between the A and B fiber for the course of 6.5 hrs in m s^{-1} , measured using UAr HCL's spectra acquired in both the fibers, wavelength calibrated with our new line list, listed in Table 1. The average differential drift between the two fibers is $\sim 12 \text{ m s}^{-1}$ with a dispersion of 0.88 m s^{-1} for the mentioned duration.

the line positions listed in the U lines template. The same has been done for the ThAr spectra using the Th lines template. We have plotted the residuals in fig 7. The standard deviation of the residuals for ThAr and UAr spectrum is found to be 0.74 and 0.81 mÅ , respectively and, the difference

between the two is within the photon noise error limit. The dispersion of the residuals from UAr spectrum is within the $3\text{-}\sigma$ of the average measurement uncertainty associated with the final U line list.

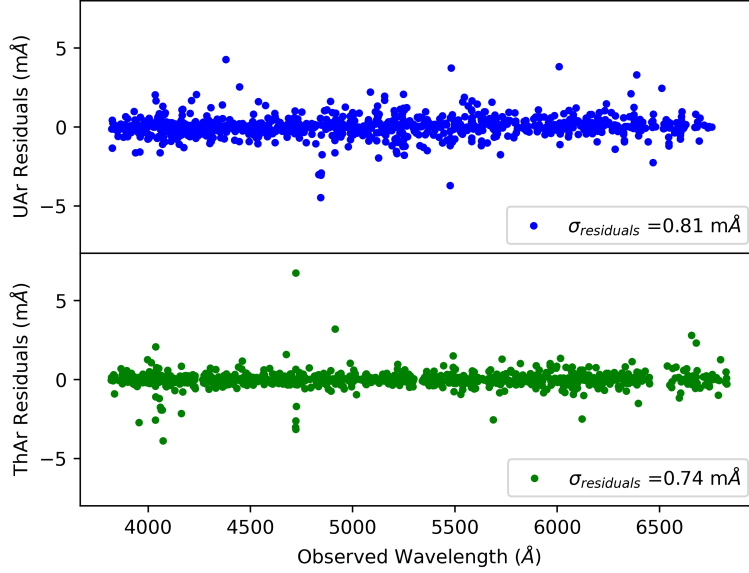


Fig 7: The plot here shows the residuals between the observed central wavelength of a random UAr spectrum and the central wavelength from the line list for UAr in the upper panel and the same for ThAr in the lower panel using Th lines. The dispersion of the residuals to the wavelength solution is 0.81 mÅ for UAr, while 0.74 mÅ for ThAr. The dispersion for UAr residuals is within the 3σ of the average measurement uncertainty (Fig 5).

6.2 The RV precision achievable on HD55575 with UAr HCL

After successfully testing the HCL with the instrument and off-sky drift measurements, we did an on-sky test with a well-known RV standard star, HD55575,²⁴ which has shown the RV dispersion of 3.4 m s^{-1} over the span of 118 days with SOPHIE+²⁴ and 3.1 m s^{-1} with PARAS using Th lines,¹³ over the span of 420 days. We observed HD55575 for the span of ~ 450 days, acquiring 27 spectra, simultaneously with the UAr HCL. The same U-lines template is used for the wavelength calibration of the extracted stellar spectra, which is used in Sec 6.1. We imposed the wavelength solution of the simultaneously acquired UAr spectra over the stellar spectra. The instrumental drift in both the fibers is corrected using the UAr-UAr exposures taken just before and after the stellar spectra. We computed the RVs by cross-correlating the stellar spectra against the template stellar mask of a G2-type star. The mean absolute stellar RV using UAr HCL is found to be $85.7597 \pm 0.001 \text{ Km s}^{-1}$, while it was $85.7498 \pm 0.001 \text{ Km s}^{-1}$ for the stellar spectra acquired simultaneously with ThAr HCL. This corresponds to an absolute RV offset of $\sim 10 \text{ m s}^{-1}$ (0.18 mÅ at 5500 Å) between the two datasets, which can be treated as an instrumental offset between the two HCLs. This offset is very close to the offset found between our final line list and the corresponding Ritz wavelengths for U lines (Sec 4) and it is a supporting evidence of consistency between wavelength calibration systemics using Th and U lines. The relative RVs for HD55575

are plotted in fig 8, and the RV dispersion for the star is found to be 3.2 m s^{-1} by nightly binning the data for the whole span of 450 days. Previously, with the use of ThAr HCL, we have achieved a RV dispersion of 3.1 m s^{-1} over 391 days.¹³ It shows that the long-term RV dispersion measured here with UAr HCL is in good agreement with the previous measurements using ThAr HCL.

We have shown that the same level of RV precision on stars as well as the same level of wavelength calibration precision is achievable using the UAr HCLs compared to the ThAr HCLs in the PARAS spectrograph. Thus, ThAr HCLs can be replaced with the UAr HCLs for the precise wavelength calibration of a high-resolution spectrum in the visible region, in PARAS-like spectrographs for exoplanet detection work and to achieve the RV precision of $1\text{-}3 \text{ m s}^{-1}$.

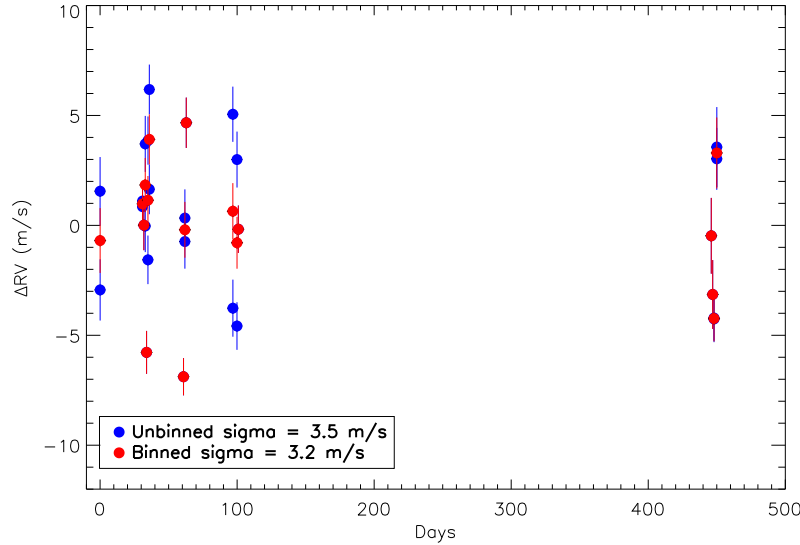


Fig 8: The plot showing relative RVs of standard star HD55575 for the span of 450 days. The blue colored data points are the RV from each observed spectra calibrated with the UAr spectra, while the red ones are the binned RV datapoints, average to each night. The dispersion of binned and unbinned RVs is 3.5 and 3.2 m s^{-1} , respectively.

7 Future works

We are planning to use the UAr HCL in our upcoming high-resolution spectrograph, PARAS-225 ($R \sim 100,000$) for instrumental characterization and wavelength calibration. The spectrograph will be attached to the upcoming PRL 2.5 meter telescope at Mount Abu Observatory, India for a goal of achieving sub- 1 m s^{-1} level of RV precision.

8 Summary

We have shown here the precise wavelength calibration of a high-resolution spectrum using U lines, acquired with the PARAS spectrograph, in the wavelength range of $3809\text{-}6833 \text{ \AA}$. We initially identified a total of 4500 line features in the UAr HCL's spectra and then filtered them through various selection steps to keep only well-resolved, well-separated, and unblended 1819 U lines. Then, we compared these lines with the closest Ritz wavelength and considered only 1540 lines for the

final line list, discarding the lines with a significantly higher difference from Ritz wavelength. The comparison showed an offset of -0.15 mÅ , with a standard deviation of 2.1 mÅ and the average wavelength measurement uncertainty of our final line list is 0.28 mÅ . We identified 160 new U transitions in this work other than the previous work of P80, and the average uncertainty in estimating the line positions in our work was found much better than that of P80. Finally, the line list was included in the PARAS data analysis framework to check the instrumental stability and RV precision. The typical dispersion of residuals in wavelength solution of a UAr spectrum is measured to be 0.8 mÅ , which is within $3\text{-}\sigma$ of mean errors in estimating the line positions. The 1σ scatter of the inter-fiber drift is found to be 88 cm s^{-1} over 6.5 hours. The stellar spectra wavelength calibrated using U lines and Th lines shows an absolute RV offset of $\sim 10 \text{ m s}^{-1}$ (0.18 mÅ at 5500 Å). This offset is a supporting evidence of consistency between wavelength calibration systemics using Th and U lines as it is in agreement with the offset our linelist from absolute wavelength scale. We measured the RV dispersion (σ_{RV}) of 3.2 m s^{-1} on a RV reference star HD55575 over the course of 450 days, using of U lines. These results are in good agreement with the previous results derived using wavelength calibration of ThAr HCL. Thus, we have demonstrated that the on-sky and off-sky acquired spectra, wavelength calibrated with the simultaneously acquired UAr HCL spectra, shows good stability in the RV and, therefore, can be used as a replacement for the ThAr HCL in the high-resolution astronomical spectrographs for precision RV measurements at a level of $1\text{--}3 \text{ m s}^{-1}$.

9 Acknowledgments

The PARAS spectrograph is fully funded and being supported by Physical Research Laboratory (PRL), which is part of Department of Space, Government of India. RS and AC would like to thank Director, PRL for his support and encouragement. RS is thankful to Priyanka Chaturvedi from TLS, Tautenburg, Germany for her valuable suggestions in improving the script and efforts in developing the various codes for analysis of the PARAS spectra. RS also acknowledges the help from Vishal Shah, Kapil Kumar, Neelam JSSV Prasad, Kevi Kumar, Ashirbad Nayak, Dishendra, Akanksha Khandelwal and Mount Abu Observatory staff at the time of observations. AC is grateful to Suvrath Mahadevan and Arpita Roy from Pennsylvania University, USA, for their tremendous efforts in developing the PARAS data pipeline in 2014.

References

- 1 D. Rouan, A. Baglin, E. Copet, *et al.*, “The Exosolar Planets Program of the COROT satellite,” *Earth Moon and Planets* **81**, 79–82 (1998).
- 2 W. J. Borucki, D. Koch, G. Basri, *et al.*, “Kepler Planet-Detection Mission: Introduction and First Results,” *Science* **327**, 977 (2010).
- 3 G. R. Ricker, J. N. Winn, R. Vanderspek, *et al.*, “Transiting Exoplanet Survey Satellite (TESS),” *Journal of Astronomical Telescopes, Instruments, and Systems* **1**, 014003 (2015).
- 4 D. L. Pollacco, I. Skillen, A. C. Cameron, *et al.*, “The WASP project and the SuperWASP cameras,” *Publications of the Astronomical Society of the Pacific* **118**, 1407–1418 (2006).
- 5 J. Pepper, R. W. Pogge, D. L. DePoy, *et al.*, “The kilodegree extremely little telescope (KELT): A small robotic telescope for large-area synoptic surveys,” *Publications of the Astronomical Society of the Pacific* **119**, 923–935 (2007).

- 6 C. Jurgenson, D. Fischer, T. McCracken, *et al.*, “EXPRES: a next generation RV spectrograph in the search for earth-like worlds,” in *Ground-based and Airborne Instrumentation for Astronomy VI*, C. J. Evans, L. Simard, and H. Takami, Eds., *Society of Photo-Optical Instrumentation Engineers (SPIE) Conference Series* **9908**, 99086T (2016).
- 7 F. Pepe, P. Molaro, S. Cristiani, *et al.*, “ESPRESSO: The next European exoplanet hunter,” *arXiv e-prints*, , arXiv:1401.5918 (2014).
- 8 T. Wilken, G. L. Curto, R. A. Probst, *et al.*, “A spectrograph for exoplanet observations calibrated at the centimetre-per-second level,” *Nature*, **485**, 611–614 (2012).
- 9 A. J. Metcalf, T. Anderson, C. F. Bender, *et al.*, “Stellar spectroscopy in the near-infrared with a laser frequency comb,” *Optica*, **6**, 233 (2019).
- 10 G. Lo Curto, L. Pasquini, A. Manescau, *et al.*, “Astronomical Spectrograph Calibration at the Exo-Earth Detection Limit,” *The Messenger* **149**, 2–6 (2012).
- 11 F. Kerber, G. Nave, C. J. Sansonetti, *et al.*, “The Spectrum of Th-Ar Hollow Cathode Lamps in the 900-4500 nm Region: Establishing Wavelength Standards for the Calibration of VLT Spectrographs,” in *The Future of Photometric, Spectrophotometric and Polarimetric Standardization*, C. Sterken, Ed., *Astronomical Society of the Pacific Conference Series* **364**, 461 (2007).
- 12 A. Chakraborty, S. Mahadevan, A. Roy, *et al.*, “The PRL Stabilized High-Resolution Echelle Fiber-fed Spectrograph: Instrument Description and First Radial Velocity Results,” *PASP*, **126**, 133 (2014).
- 13 A. Chakraborty, A. Roy, R. Sharma, *et al.*, “Evidence of a Sub-Saturn around EPIC 211945201,” *The Astronomical Journal*, **156**, 3 (2018).
- 14 X. Dumusque, F. Pepe, C. Lovis, *et al.*, “An Earth-mass planet orbiting α Centauri B,” *Nature*, **491**, 207–211 (2012).
- 15 G. Nave, F. Kerber, E. A. Den Hartog, *et al.*, “The dirt in astronomy’s genie lamp: ThO contamination of Th-Ar calibration lamps,” *Proceedings of the SPIE*, **10704**, 1070407 (2018).
- 16 S. L. Redman, G. G. Ycas, R. Terrien, *et al.*, “A High-resolution Atlas of Uranium-Neon in the H Band,” *The Astrophysical Journal Supplement Series*, **199**, 2 (2012).
- 17 L. F. Sarmiento, A. Reiners, P. Huke, *et al.*, “Comparing the emission spectra of U and Th hollow cathode lamps and a new U line list,” *Astronomy and Astrophysics*, **618**, A118 (2018).
- 18 B. A. Palmer, R. A. Keller, and J. Engleman, Rolf, “Atlas of uranium emission intensities in a hollow cathode discharge,” *Los Alamos Scientific Laboratory*, **12**, Report number LA–8251–MS (1980).
- 19 N. E. Piskunov and J. A. Valenti, “New algorithms for reducing cross-dispersed echelle spectra,” *Astronomy and Astrophysics*, **385**, 1095–1106 (2002).
- 20 C. B. Markwardt, *Non-linear Least-squares Fitting in IDL with MPFIT*, vol. 411 of *Astronomical Society of the Pacific Conference Series*, , 251 (2009).
- 21 C. Lovis and F. Pepe, “A new list of thorium and argon spectral lines in the visible,” *Astronomy and Astrophysics*, **468**, 1115–1121 (2007).
- 22 S. L. Redman, G. Nave, and C. J. Sansonetti, “The Spectrum of Thorium from 250 nm to 5500 nm: Ritz Wavelengths and Optimized Energy Levels,” *The Astrophysical Journal Supplement Series*, **211**, 4 (2014).

- 23 F. Bouchy, F. Pepe, and D. Queloz, “Fundamental photon noise limit to radial velocity measurements,” *Astronomy and Astrophysics*, **374**, 733–739 (2001).
- 24 F. Bouchy, R. F. Díaz, G. Hébrard, *et al.*, “SOPHIE+: First results of an octagonal-section fiber for high-precision radial velocity measurements,” *Astronomy and Astrophysics*, **549**, A49 (2013).
- 25 A. Chakraborty, N. Thapa, K. Kumar, *et al.*, “PARAS-2 precision radial velocimeter: optical and mechanical design of a fiber-fed high resolution spectrograph under vacuum and temperature control,” in *Ground-based and Airborne Instrumentation for Astronomy VII*, C. J. Evans, L. Simard, and H. Takami, Eds., **10702**, 1967 – 1978, International Society for Optics and Photonics, SPIE (2018).

Table 1: The final line list of uranium from PARAS spectrograph.

Observed Wavelength Å	Ritz Wavelength Å	Relative Flux ADU	Uncertainty mÅ	Offset from Ritz wavelength mÅ	Species	Source
3809.4663	3809.4617	6153	0.2709	4.6000	UII	RS21
3821.9472	3821.9467	2900	0.3183	0.5353	UI	RS21
3824.5337	3824.5374	4240	0.2671	-3.7387	UI	RS21
3829.7954	3829.7935	2885	0.3030	1.9979	UI	RS21
3831.8545	3831.8509	2295	0.3486	3.5569	UI	RS21
3835.2266	3835.2240	4017	0.2662	2.6342	UI	RS21
3839.6262	3839.6267	16468	0.1219	-0.5369	UI	RS21
3844.9362	3844.9361	4423	0.2621	0.0783	UI	RS21
3846.2336	3846.2340	2320	0.3695	-0.3674	UI	RS21
3846.5552	3846.5531	6241	0.2008	2.1042	UI	RS21
3847.8352	3847.8333	2744	0.3293	1.9423	UI	RS21
3849.8459	3849.8464	2730	0.3671	-0.4852	UII	P80
3850.3220	3850.3234	2932	0.3877	-1.3760	UI	P80
3851.7208	3851.7266	3616	0.3706	-5.8155	UI	P80
3854.2204	3854.2198	55600	0.0623	0.5819	UI	P80
3854.6435	3854.6442	9367	0.1687	-0.6617	UII	P80
3855.4299	3855.4278	5576	0.2356	2.1020	UI	P80
3859.0029	3859.0075	3052	0.3462	-4.5976	UII	P80
3859.5742	3859.5714	33465	0.0830	2.7509	UII	P80
3863.0985	3863.1017	4407	0.2660	-3.1962	UII	P80
3865.9207	3865.9168	10298	0.1585	3.9189	UII	P80
3867.1734	3867.1719	4884	0.2469	1.5081	UI	P80
3868.6937	3868.6968	4885	0.3230	-3.0404	UI	P80
3871.0370	3871.0348	96319	0.0474	2.2192	UI	P80
3873.0805	3873.0791	6808	0.1901	1.3670	UI	P80
3874.3545	3874.3515	5922	0.2339	3.0527	UI	P80
3876.1317	3876.1327	26779	0.0902	-1.0274	UI	P80
3878.4534	3878.4536	3451	0.3964	-0.2127	UI	P80

continued ...

Observed Wavelength Å	Ritz Wavelength Å	Relative Flux ADU	Uncertainty mÅ	Offset from Ritz wavelength mÅ	Species	Source
3879.5363	3879.5345	3890	0.2863	1.8200	UI	P80
3879.7099	3879.7107	3731	0.2939	-0.7282	UI	P80
3881.4516	3881.4539	3709	0.2861	-2.2699	UII	P80
3882.3555	3882.3556	3272	0.3372	-0.0850	UII	P80
3883.1103	3883.1114	2566	0.3941	-1.1444	UI	P80
3883.6339	3883.6350	2528	0.4096	-1.1069	UI	P80
3887.4411	3887.4397	3127	0.3242	1.3727	UI	P80
3889.2835	3889.2785	4661	0.2769	5.0163	UI	P80
3890.3630	3890.3613	22125	0.1096	1.7274	UII	P80
3891.8020	3891.8019	6755	0.2195	0.0778	UI	P80
3892.6830	3892.6809	5293	0.2340	2.0157	UII	P80
3892.8935	3892.8920	2896	0.3529	1.4235	UI	P80
3893.7162	3893.7147	3146	0.3679	1.5331	UII	P80
3894.1212	3894.1206	62820	0.0591	0.6696	UI	P80
3894.9058	3894.9032	6980	0.1982	2.6250	UI	P80
3895.2662	3895.2698	2939	0.3420	-3.6473	UII	P80
3895.7176	3895.7160	3066	0.3285	1.5505	UI	P80
3896.7749	3896.7745	3859	0.3028	0.3755	UII	P80
3897.2676	3897.2611	3842	0.3150	6.4362	UII	P80
3899.2692	3899.2702	6389	0.1964	-1.0529	UI	P80
3899.4720	3899.4731	3350	0.3276	-1.1083	UII	P80
3899.7816	3899.7806	6000	0.2522	1.0188	UII	P80
3915.2104	3915.2104	6471	0.2065	0.0176	UI	P80
3916.3436	3916.3398	3114	0.3431	3.8548	UI	P80
3916.5205	3916.5205	4298	0.2983	0.0137	UI	P80
3921.5485	3921.5475	3733	0.2963	0.9701	UII	P80
3923.0248	3923.0215	9463	0.1679	3.2665	UI	P80
3924.2568	3924.2604	2407	0.3861	-3.6242	UII	P80
3926.2087	3926.2077	32720	0.0834	0.9985	UI	P80

continued ...

Observed Wavelength Å	Ritz Wavelength Å	Relative Flux ADU	Uncertainty mÅ	Offset from Ritz wavelength mÅ	Species	Source
3928.8245	3928.8245	13038	0.1376	0.0104	UI	P80
3931.5050	3931.5069	3273	0.3258	-1.9663	UI	P80
3932.0230	3932.0222	25576	0.0982	0.8433	UII	P80
3935.3795	3935.3800	4920	0.2396	-0.5082	UII	P80
3938.3521	3938.3521	3383	0.3123	0.0233	UII	RS21
3940.4848	3940.4839	3334	0.3372	0.9542	UII	P80
3943.8175	3943.8161	92109	0.0476	1.4197	UI	P80
3944.2723	3944.2719	10163	0.1682	0.3755	UI	RS21
3948.4440	3948.4428	19971	0.1284	1.1676	UI	P80
3948.6595	3948.6555	2842	0.3618	4.0735	UI	P80
3948.9821	3948.9863	26235	0.0969	-4.2098	UI	P80
3950.4764	3950.4731	5519	0.2354	3.3499	UI	P80
3951.4756	3951.4734	4246	0.3075	2.2387	UI	P80
3959.2074	3959.2058	2985	0.3467	1.5410	UI	P80
3960.6566	3960.6565	2558	0.3776	0.1379	UI	P80
3961.5097	3961.5123	14069	0.1518	-2.6019	UI	P80
3962.8003	3962.8054	4970	0.2612	-5.1351	UI	P80
3967.4634	3967.4624	16186	0.1192	0.9970	UI	P80
3969.4134	3969.4119	12953	0.1288	1.5715	UI	P80
3970.5871	3970.5869	7174	0.1945	0.1748	UI	P80
3972.2125	3972.2124	9879	0.1634	0.1236	UI	P80
3980.7976	3980.7955	3882	0.2887	2.1222	UI	P80
3983.7723	3983.7686	3166	0.3387	3.7075	UI	P80
3985.7944	3985.7919	6884	0.1976	2.5050	UII	P80
3988.8868	3988.8838	3337	0.3115	3.0776	UII	P80
3989.2897	3989.2885	2837	0.3519	1.1572	UI	P80
3990.4222	3990.4203	9220	0.1643	1.8844	UII	P80
3992.5322	3992.5344	3067	0.3515	-2.2677	UII	P80
3992.8416	3992.8384	2761	0.3967	3.2360	UI	P80

continued ...

Observed Wavelength Å	Ritz Wavelength Å	Relative Flux ADU	Uncertainty mÅ	Offset from Ritz wavelength mÅ	Species	Source
3994.2909	3994.2907	2803	0.3450	0.1388	UII	P80
3997.0841	3997.0812	4730	0.2314	2.9699	UI	RS21
3999.1817	3999.1798	10199	0.1493	1.8472	UI	P80
4001.2808	4001.2798	5307	0.2894	1.0262	UI	P80
4002.5878	4002.5883	2859	0.3561	-0.5652	UI	P80
4002.9844	4002.9834	2819	0.3681	1.0715	UI	P80
4005.2075	4005.2089	39252	0.0824	-1.3937	UI	P80
4005.6953	4005.6948	22761	0.1022	0.5395	UI	P80
4010.8131	4010.8124	3119	0.3138	0.7723	UI	P80
4014.8084	4014.8056	3898	0.2865	2.8439	UI	P80
4015.2361	4015.2352	3641	0.2999	0.9831	UI	P80
4017.7161	4017.7159	3885	0.2794	0.1697	UII	P80
4018.2971	4018.2963	3334	0.3011	0.8709	UI	P80
4024.2476	4024.2487	2829	0.3474	-1.0430	UI	P80
4026.0228	4026.0225	9948	0.1579	0.2604	UII	P80
4031.8056	4031.8054	3333	0.3073	0.2001	UI	P80
4034.4956	4034.4965	7097	0.1958	-0.8863	UI	P80
4037.9678	4037.9680	3570	0.3004	-0.2884	UI	P80
4040.6955	4040.6923	9154	0.1814	3.2748	UI	P80
4042.7511	4042.7495	82979	0.0626	1.5411	UI	P80
4044.8963	4044.8942	2843	0.3804	2.0932	UI	P80
4047.6127	4047.6114	76397	0.0539	1.2468	UI	P80
4049.1890	4049.1878	6043	0.2075	1.1429	UI	P80
4049.7746	4049.7744	4387	0.2710	0.1906	UI	P80
4050.0451	4050.0414	30133	0.0944	3.7120	UII	P80
4051.9136	4051.9112	7528	0.1895	2.3832	UII	P80
4054.3022	4054.3035	3555	0.3549	-1.3118	UI	P80
4054.6751	4054.6732	12407	0.1459	1.8535	UI	P80
4055.9449	4055.9401	3293	0.4095	4.8537	UI	P80

continued ...

Observed Wavelength Å	Ritz Wavelength Å	Relative Flux ADU	Uncertainty mÅ	Offset from Ritz wavelength mÅ	Species	Source
4061.3483	4061.3494	21637	0.1025	-1.1034	UII	P80
4062.3212	4062.3186	13783	0.1342	2.5594	UI	P80
4062.5432	4062.5443	21435	0.1092	-1.0915	UII	P80
4063.0904	4063.0896	5069	0.2373	0.7706	UI	P80
4064.0236	4064.0213	2395	0.3931	2.2850	UI	P80
4066.2889	4066.2872	8104	0.1943	1.6848	UI	P80
4067.7473	4067.7475	5030	0.2390	-0.1852	UII	P80
4068.6997	4068.7004	3548	0.3374	-0.7485	UI	P80
4069.6472	4069.6454	5160	0.2314	1.7919	UI	P80
4070.0075	4070.0065	8355	0.1675	0.9405	UI	P80
4070.4439	4070.4438	5095	0.2555	0.0777	UI	P80
4070.8834	4070.8850	12858	0.1489	-1.6052	UI	P80
4072.8304	4072.8322	3083	0.3682	-1.8050	UI	P80
4073.5409	4073.5401	8841	0.1740	0.8417	UI	P80
4074.6142	4074.6131	12131	0.1557	1.0792	UI	P80
4075.8961	4075.8938	4589	0.2713	2.2834	UI	P80
4077.7852	4077.7850	15579	0.1241	0.2077	UI	P80
4081.2134	4081.2172	4625	0.3023	-3.7802	UI	P80
4082.8220	4082.8202	7129	0.2056	1.8444	UI	P80
4083.0315	4083.0374	13227	0.1463	-5.9123	UI	P80
4084.0974	4084.0962	13344	0.1374	1.1852	UI	P80
4088.2553	4088.2521	4453	0.2639	3.1249	UI	P80
4089.1549	4089.1542	5711	0.2175	0.6903	UI	P80
4090.1324	4090.1326	25864	0.0930	-0.1872	UII	P80
4091.6275	4091.6268	35994	0.0780	0.7417	UI	P80
4094.8856	4094.8900	2316	0.4248	-4.4720	UII	P80
4096.3519	4096.3500	10411	0.1572	1.8430	UI	P80
4097.7450	4097.7438	17256	0.1164	1.2025	UI	P80
4098.0258	4098.0243	9654	0.2045	1.4743	UII	P80

continued ...

Observed Wavelength Å	Ritz Wavelength Å	Relative Flux ADU	Uncertainty mÅ	Offset from Ritz wavelength mÅ	Species	Source
4098.9868	4098.9842	2643	0.3917	2.5279	UI	P80
4101.9061	4101.9045	15451	0.1257	1.5856	UI	P80
4103.1126	4103.1123	16104	0.1251	0.3761	UI	P80
4104.9452	4104.9458	8399	0.1873	-0.5851	UI	P80
4105.3163	4105.3100	5871	0.2267	6.2962	UI	P80
4106.9277	4106.9230	7161	0.2132	4.6213	UII	P80
4107.5221	4107.5235	4915	0.2994	-1.4795	UII	P80
4108.3527	4108.3524	29849	0.0889	0.3424	UI	P80
4109.5343	4109.5342	2694	0.3879	0.0590	UI	P80
4109.6987	4109.6982	2493	0.3965	0.4722	UI	P80
4110.6416	4110.6458	3824	0.3299	-4.2309	UI	P80
4110.8323	4110.8300	2550	0.4180	2.3011	UII	P80
4111.0173	4111.0182	8588	0.1729	-0.9373	UI	P80
4115.6440	4115.6444	4731	0.2431	-0.3674	UI	P80
4116.0963	4116.0975	23429	0.0995	-1.1642	UII	P80
4116.3471	4116.3428	10004	0.1905	4.2799	UI	P80
4116.8839	4116.8818	5371	0.2529	2.1227	UII	P80
4122.1675	4122.1698	3118	0.3430	-2.3005	UI	P80
4122.3563	4122.3567	6219	0.2197	-0.4021	UI	P80
4122.9987	4122.9962	3478	0.3182	2.5027	UI	P80
4124.7272	4124.7273	11683	0.1525	-0.0623	UII	P80
4125.1305	4125.1298	7785	0.1848	0.6802	UI	P80
4127.3339	4127.3359	5378	0.2469	-2.0101	UII	P80
4127.5530	4127.5502	3036	0.6602	2.8107	UII	P80
4128.3350	4128.3345	12773	0.1352	0.4481	UII	P80
4130.6617	4130.6587	6083	0.2294	3.0296	UI	P80
4131.7247	4131.7253	420538	0.0229	-0.6646	UI	RS21
4132.0111	4132.0102	7096	0.2701	0.8932	UI	P80
4133.2037	4133.2007	4216	0.3026	3.0322	UII	P80

continued ...

Observed Wavelength Å	Ritz Wavelength Å	Relative Flux ADU	Uncertainty mÅ	Offset from Ritz wavelength mÅ	Species	Source
4133.4924	4133.4911	79374	0.0548	1.3487	UI	P80
4135.7563	4135.7552	3423	0.4522	1.1108	UII	P80
4137.0387	4137.0335	3715	0.3941	5.2087	UI	P80
4137.7157	4137.7134	3233	0.3763	2.3561	UI	P80
4138.6591	4138.6585	3530	0.3427	0.5651	UII	P80
4138.9611	4138.9621	4959	0.2665	-0.9847	UI	P80
4139.1405	4139.1388	10870	0.1694	1.7334	UII	P80
4141.8590	4141.8579	40662	0.0724	1.1952	UI	P80
4146.6154	4146.6149	5307	0.2278	0.5730	UI	RS21
4148.0346	4148.0293	3129	0.2989	5.2972	UI	P80
4166.6391	4166.6449	2481	0.3845	-5.7460	UII	P80
4169.0473	4169.0473	2878	0.3527	-0.0133	UI	P80
4171.5913	4171.5889	11288	0.1478	2.4195	UII	P80
4176.4568	4176.4561	3613	0.2950	0.7478	UI	P80
4179.0044	4179.0029	2962	0.4095	1.4407	UII	P80
4179.2991	4179.3025	21653	0.1199	-3.4035	UII	RS21
4180.3063	4180.3053	24353	0.0938	1.0006	UI	P80
4182.9634	4182.9663	5357	0.2698	-2.9225	UI	RS21
4183.2598	4183.2572	5870	0.2252	2.5900	UI	P80
4184.7716	4184.7727	2922	0.6583	-1.1195	UI	P80
4186.9601	4186.9604	33207	0.0845	-0.3249	UI	P80
4188.0645	4188.0639	9100	0.1741	0.6035	UII	P80
4188.8884	4188.8910	3858	0.3203	-2.6071	UII	P80
4189.6511	4189.6566	5571	0.2596	-5.5697	UI	RS21
4191.9334	4191.9326	36889	0.0785	0.7760	UI	P80
4192.9063	4192.9099	5137	0.2602	-3.5429	UI	P80
4195.6134	4195.6120	3076	0.3844	1.4125	UI	P80
4196.3983	4196.3997	4388	0.3086	-1.4129	UI	P80
4198.3130	4198.3131	143729	0.0521	-0.1487	UII	RS21

continued ...

Observed Wavelength Å	Ritz Wavelength Å	Relative Flux ADU	Uncertainty mÅ	Offset from Ritz wavelength mÅ	Species	Source
4199.6274	4199.6252	3634	0.3089	2.1707	UI	P80
4201.1266	4201.1260	7929	0.1895	0.5670	UI	P80
4203.4112	4203.4127	2345	0.4245	-1.4916	UII	RS21
4204.1628	4204.1616	4472	0.2455	1.1876	UI	P80
4204.3480	4204.3529	2742	0.3667	-4.8808	UII	P80
4222.3630	4222.3675	5414	0.2252	-4.5775	UI	P80
4228.4238	4228.4237	6067	0.2268	0.1198	UII	P80
4229.8687	4229.8651	3545	0.3616	3.6115	UII	RS21
4231.6689	4231.6682	10726	0.1682	0.7750	UI	P80
4232.0338	4232.0373	3598	0.3294	-3.4934	UI	P80
4233.1318	4233.1321	8606	0.1705	-0.3057	UI	P80
4233.5471	4233.5431	3744	0.3185	4.0053	UI	P80
4236.0261	4236.0301	7775	0.2172	-3.9653	UII	P80
4241.1089	4241.1117	15609	0.1259	-2.8093	UI	P80
4241.6651	4241.6642	22140	0.1011	0.8365	UII	P80
4244.3731	4244.3726	34111	0.0841	0.5880	UII	P80
4246.2601	4246.2599	142241	0.0399	0.2158	UI	P80
4247.9011	4247.9003	5131	0.2563	0.8143	UI	P80
4252.4263	4252.4265	4662	0.2650	-0.1880	UII	P80
4253.7059	4253.7054	2672	0.4015	0.4809	UI	P80
4266.3051	4266.3016	53946	0.0778	3.4819	UI	P80
4267.2994	4267.2989	4163	0.2812	0.4981	UII	P80
4268.8487	4268.8471	4153	0.2604	1.6623	UII	P80
4269.6077	4269.6094	9727	0.1615	-1.7265	UII	P80
4271.2289	4271.2281	13114	0.1461	0.8517	UI	P80
4272.1702	4272.1735	72105	0.0575	-3.3154	UI	RS21
4273.9709	4273.9711	5083	0.2238	-0.1614	UII	P80
4277.5283	4277.5311	478484	0.0212	-2.8064	UII	RS21
4279.3244	4279.3235	3350	0.3257	0.8632	UI	P80

continued ...

Observed Wavelength Å	Ritz Wavelength Å	Relative Flux ADU	Uncertainty mÅ	Offset from Ritz wavelength mÅ	Species	Source
4280.0346	4280.0338	2794	0.4037	0.8481	UI	P80
4281.2206	4281.2234	2706	0.4989	-2.8111	UI	P80
4282.0238	4282.0232	13404	0.1398	0.5774	UII	P80
4283.9049	4283.8997	3284	0.3303	5.2514	UI	P80
4285.2279	4285.2285	2875	0.3403	-0.5553	UI	P80
4287.8647	4287.8613	6983	0.2317	3.3968	UII	P80
4288.8378	4288.8349	17388	0.1193	2.9096	UII	P80
4297.1083	4297.1098	6575	0.2133	-1.5281	UI	P80
4301.4647	4301.4635	9400	0.1721	1.1284	UII	P80
4301.7121	4301.7122	3216	0.3177	-0.1042	UI	P80
4306.8115	4306.8133	21289	0.1148	-1.7741	UI	P80
4308.1977	4308.1970	3281	0.2919	0.6629	UI	P80
4309.6900	4309.6882	23461	0.1024	1.7770	UI	P80
4313.1379	4313.1386	34650	0.0864	-0.7197	UI	P80
4313.8722	4313.8737	7091	0.2141	-1.4825	UII	P80
4316.4836	4316.4828	4509	0.2609	0.8415	UI	P80
4317.0693	4317.0697	3626	0.2966	-0.3296	UI	P80
4318.0881	4318.0905	3314	0.3312	-2.3920	UI	P80
4322.3807	4322.3821	5974	0.2201	-1.3734	UI	P80
4325.0889	4325.0892	3316	0.3163	-0.3122	UII	P80
4325.8862	4325.8839	2953	0.3471	2.2576	UII	P80
4328.7304	4328.7298	24371	0.0992	0.5752	UI	P80
4331.4390	4331.4438	5961	0.2635	-4.7961	UI	P80
4335.7330	4335.7315	61394	0.0613	1.4952	UI	P80
4337.3983	4337.3981	11081	0.1491	0.2326	UI	P80
4337.6266	4337.6267	2706	0.3661	-0.0866	UI	P80
4341.6865	4341.6869	38605	0.0792	-0.3227	UII	P80
4345.1682	4345.1725	15160	0.1327	-4.2407	UII	RS21
4347.1939	4347.1956	5680	0.2384	-1.6234	UII	P80

continued ...

Observed Wavelength Å	Ritz Wavelength Å	Relative Flux ADU	Uncertainty mÅ	Offset from Ritz wavelength mÅ	Species	Source
4354.5474	4354.5487	8623	0.1852	-1.3217	UII	P80
4355.7401	4355.7393	102224	0.0499	0.7956	UI	P80
4357.9149	4357.9136	10413	0.1558	1.2501	UI	P80
4362.0529	4362.0513	271630	0.0286	1.6487	UI	P80
4362.2577	4362.2602	23774	0.1179	-2.4479	UII	P80
4363.1819	4363.1816	3908	0.3350	0.2450	UI	P80
4364.4128	4364.4105	2863	0.3234	2.2664	UI	P80
4367.8323	4367.8332	32311	0.0946	-0.9096	UI	RS21
4369.9542	4369.9528	6263	0.2278	1.3762	UI	P80
4370.7539	4370.7592	183551	0.0386	-5.2305	UII	RS21
4371.7586	4371.7585	17779	0.1231	0.0495	UI	P80
4372.0077	4372.0054	9519	0.1918	2.3719	UI	P80
4372.5663	4372.5656	14656	0.1823	0.6700	UI	P80
4372.7559	4372.7554	88012	0.0524	0.5269	UI	P80
4373.4046	4373.4029	8412	0.2032	1.7413	UI	P80
4382.0700	4382.0692	4129	0.2842	0.8735	UI	P80
4382.3363	4382.3359	18955	0.1126	0.3512	UI	RS21
4382.8425	4382.8388	2546	0.4586	3.7200	UI	P80
4383.2617	4383.2617	17549	0.1201	-0.0792	UI	P80
4387.3113	4387.3104	8639	0.1785	0.8882	UI	P80
4392.4979	4392.5024	4166	0.2999	-4.5509	UI	P80
4393.5860	4393.5857	252206	0.0293	0.3146	UI	P80
4400.9864	4400.9809	130467	0.0452	5.4851	UI	RS21
4413.1334	4413.1336	6656	0.2045	-0.1968	UI	P80
4415.2366	4415.2376	5508	0.2458	-1.0681	UII	P80
4418.4723	4418.4727	4281	0.2653	-0.4116	UI	P80
4422.9889	4422.9853	2795	0.3717	3.5666	UII	P80
4425.4093	4425.4091	7700	0.2043	0.2784	UI	P80
4426.0014	4425.9984	335096	0.0275	3.0387	UI	RS21

continued ...

Observed Wavelength Å	Ritz Wavelength Å	Relative Flux ADU	Uncertainty mÅ	Offset from Ritz wavelength mÅ	Species	Source
4426.9350	4426.9343	80768	0.0519	0.6345	UI	P80
4427.6517	4427.6523	6844	0.2062	-0.6427	UII	P80
4429.6144	4429.6142	2794	0.4287	0.2195	UII	P80
4431.8688	4431.8668	3895	0.2746	2.0791	UI	P80
4434.5321	4434.5315	13991	0.1392	0.6489	UII	P80
4434.9038	4434.8980	2839	0.4332	5.7817	UI	P80
4440.7377	4440.7369	21065	0.1111	0.8130	UI	P80
4441.0815	4441.0782	3892	0.3832	3.2060	UII	P80
4444.6839	4444.6840	4259	0.2715	-0.1162	UI	P80
4446.5173	4446.5216	3155	0.4331	-4.3102	UI	P80
4447.0430	4447.0408	3468	0.3260	2.2299	UI	P80
4448.3327	4448.3305	8949	0.1885	2.2649	UI	P80
4452.9306	4452.9303	2553	0.4140	0.2819	UI	P80
4453.2128	4453.2119	8478	0.1755	0.9098	UI	P80
4457.4526	4457.4526	6591	0.2072	-0.0301	UI	P80
4458.7016	4458.7014	31712	0.0882	0.1967	UI	P80
4461.4434	4461.4451	7309	0.2010	-1.7806	UI	P80
4462.9681	4462.9685	8477	0.1756	-0.3423	UII	P80
4469.3247	4469.3248	58129	0.0653	-0.0812	UI	P80
4472.3309	4472.3298	35913	0.0828	1.1140	UII	P80
4476.4715	4476.4676	6281	0.2249	3.8925	UI	P80
4490.8336	4490.8318	7738	0.2428	1.7488	UII	P80
4492.6400	4492.6395	4446	0.2638	0.5060	UI	P80
4493.0423	4493.0410	2834	0.4082	1.2758	UII	P80
4494.7124	4494.7115	33187	0.0818	0.8755	UI	P80
4510.0915	4510.0912	6098	0.2252	0.3444	UI	RS21
4510.7329	4510.7299	38078	0.0843	2.9858	UI	RS21
4515.2752	4515.2773	13710	0.1445	-2.0497	UII	P80
4515.9803	4515.9764	2544	0.4225	3.9183	UI	P80

continued ...

Observed Wavelength Å	Ritz Wavelength Å	Relative Flux ADU	Uncertainty mÅ	Offset from Ritz wavelength mÅ	Species	Source
4516.7242	4516.7228	44413	0.0752	1.3735	UI	P80
4520.0783	4520.0781	6829	0.1964	0.2244	UI	RS21
4522.3234	4522.3273	9060	0.1828	-3.9414	UI	RS21
4523.3393	4523.3444	2640	0.3988	-5.0741	UII	P80
4526.2454	4526.2464	2397	0.3989	-1.0407	UI	P80
4527.6918	4527.6926	2728	0.3563	-0.8066	UI	P80
4529.7057	4529.7032	2615	0.3756	2.4629	UI	P80
4531.1373	4531.1368	4795	0.2793	0.5283	UI	P80
4532.5809	4532.5805	12716	0.1506	0.4460	UI	P80
4536.6007	4536.6014	6316	0.2243	-0.6558	UI	P80
4538.1799	4538.1854	9554	0.1973	-5.4317	UI	P80
4539.0771	4539.0772	3342	0.3333	-0.1093	UI	P80
4541.3277	4541.3276	6311	0.2270	0.0464	UI	P80
4541.7076	4541.7112	2309	0.4641	-3.6653	UI	P80
4543.6248	4543.6259	29563	0.0958	-1.0688	UII	P80
4544.3529	4544.3548	7208	0.2146	-1.8403	UI	P80
4545.5921	4545.5962	50833	0.0740	-4.1235	UI	P80
4546.0862	4546.0875	2522	0.4555	-1.3532	UII	P80
4550.9772	4550.9764	3231	0.3628	0.8073	UI	P80
4551.5725	4551.5725	12962	0.1454	-0.0069	UI	P80
4551.9739	4551.9744	50892	0.0698	-0.4842	UI	P80
4553.8525	4553.8540	6397	0.2257	-1.4475	UII	P80
4555.0887	4555.0896	3212	0.3608	-0.8786	UII	P80
4558.0425	4558.0422	13677	0.1380	0.2820	UI	P80
4559.6429	4559.6428	16654	0.1253	0.1297	UI	P80
4566.5082	4566.5042	2864	0.5103	4.0395	UI	P80
4567.6844	4567.6848	15658	0.1341	-0.3471	UII	P80
4569.9092	4569.9090	18341	0.1232	0.2135	UI	P80
4571.6821	4571.6767	2632	0.4662	5.3041	UI	P80

continued ...

Observed Wavelength Å	Ritz Wavelength Å	Relative Flux ADU	Uncertainty mÅ	Offset from Ritz wavelength mÅ	Species	Source
4573.2731	4573.2731	2534	0.4529	0.0080	UII	P80
4573.5193	4573.5195	3214	0.4136	-0.1249	UII	P80
4573.6778	4573.6797	11833	0.1582	-1.8701	UII	P80
4575.0210	4575.0218	3729	0.3355	-0.7447	UI	P80
4576.6387	4576.6397	57549	0.0674	-0.9102	UI	P80
4578.0035	4578.0048	3352	0.3310	-1.3374	UI	P80
4579.3479	4579.3498	150888	0.0446	-1.9620	UII	RS21
4583.2880	4583.2855	2388	0.4466	2.4623	UII	P80
4584.8480	4584.8481	3917	0.3182	-0.0660	UI	P80
4585.5695	4585.5681	3841	0.3226	1.3689	UI	P80
4587.2387	4587.2391	3029	0.4909	-0.3979	UII	P80
4588.6436	4588.6431	6750	0.2115	0.5651	UI	P80
4592.6210	4592.6191	6388	0.2421	1.9134	UI	P80
4593.6388	4593.6379	4616	0.2939	0.9113	UI	P80
4594.8430	4594.8412	9073	0.1801	1.7417	UI	P80
4595.4492	4595.4468	7567	0.2241	2.3667	UI	P80
4601.1252	4601.1281	10091	0.1871	-2.9055	UII	P80
4603.4203	4603.4202	4253	0.3183	0.0618	UI	P80
4603.6590	4603.6583	16736	0.1321	0.6504	UII	P80
4608.3455	4608.3490	2676	0.4450	-3.4818	UI	P80
4618.7377	4618.7384	4138	0.2989	-0.6441	UI	P80
4620.2149	4620.2126	41990	0.0888	2.3138	UI	P80
4620.4274	4620.4278	51049	0.0738	-0.3470	UI	P80
4622.4229	4622.4219	5108	0.2768	0.9944	UII	P80
4625.4873	4625.4892	9265	0.1966	-1.9007	UI	P80
4630.8973	4630.8977	4152	0.3392	-0.4100	UI	P80
4631.6154	4631.6151	319240	0.0278	0.3288	UI	P80
4637.9368	4637.9376	5298	0.2690	-0.7166	UII	P80
4641.6551	4641.6501	2508	0.4497	5.0314	UII	P80

continued ...

Observed Wavelength Å	Ritz Wavelength Å	Relative Flux ADU	Uncertainty mÅ	Offset from Ritz wavelength mÅ	Species	Source
4643.6032	4643.6023	10032	0.1780	0.8401	UI	P80
4646.5982	4646.5974	17843	0.1281	0.8253	UII	P80
4654.8362	4654.8333	3670	0.3422	2.8894	UII	P80
4657.9019	4657.9039	479801	0.0237	-2.0492	UI	RS21
4660.1097	4660.1066	3103	0.4339	3.0840	UI	P80
4661.6482	4661.6464	6599	0.2401	1.7815	UI	P80
4663.7492	4663.7489	122024	0.0438	0.2982	UII	P80
4665.8161	4665.8150	18533	0.1201	1.1014	UI	P80
4666.8515	4666.8513	20562	0.1130	0.1432	UII	P80
4667.7202	4667.7195	3863	0.3732	0.6974	UII	P80
4671.3966	4671.3976	9423	0.1918	-0.9807	UII	P80
4677.5288	4677.5291	2832	0.4102	-0.3250	UI	P80
4677.7385	4677.7381	3546	0.3595	0.3915	UI	P80
4678.6681	4678.6681	2902	0.4036	-0.0262	UI	P80
4682.0065	4682.0084	12999	0.1989	-1.8978	UI	P80
4685.1912	4685.1922	4654	0.2915	-1.0520	UI	P80
4686.9218	4686.9225	22532	0.1134	-0.6524	UI	P80
4689.0739	4689.0740	25585	0.1064	-0.0914	UII	P80
4691.2519	4691.2517	4172	0.3669	0.2568	UI	P80
4693.7008	4693.6995	4447	0.3673	1.2986	UI	P80
4694.7014	4694.7008	7606	0.2111	0.5931	UI	P80
4695.2232	4695.2223	26708	0.1139	0.8276	UI	P80
4695.6382	4695.6350	5061	0.3372	3.2252	UI	P80
4696.0480	4696.0434	3167	0.4269	4.6125	UI	P80
4700.7050	4700.7050	5262	0.2869	-0.0567	UII	P80
4700.9754	4700.9753	9394	0.2242	0.1591	UII	P80
4701.2271	4701.2266	120903	0.0450	0.4738	UI	P80
4702.0395	4702.0376	6960	0.2481	1.8606	UII	P80
4702.3168	4702.3227	24057	0.1165	-5.8983	UII	RS21

continued ...

Observed Wavelength Å	Ritz Wavelength Å	Relative Flux ADU	Uncertainty mÅ	Offset from Ritz wavelength mÅ	Species	Source
4702.5114	4702.5120	12350	0.1678	-0.5244	UII	P80
4705.1363	4705.1419	3288	0.4532	-5.6276	UI	P80
4708.1588	4708.1550	6017	0.2980	3.8071	UI	P80
4709.3509	4709.3567	4045	0.3855	-5.7865	UI	P80
4710.8143	4710.8156	4050	0.3694	-1.2932	UI	P80
4712.1366	4712.1323	2633	0.8236	4.3051	UII	P80
4713.9352	4713.9328	3472	0.4134	2.4271	UI	P80
4715.6677	4715.6695	11543	0.1837	-1.8198	UI	P80
4717.8302	4717.8306	6762	0.2560	-0.4436	UI	P80
4722.7178	4722.7174	20983	0.1270	0.4715	UII	P80
4727.1091	4727.1078	12296	0.2531	1.3088	UII	P80
4727.3361	4727.3370	11271	0.1860	-0.8590	UI	P80
4727.6580	4727.6579	22208	0.1283	0.1176	UI	P80
4730.6760	4730.6746	57449	0.0714	1.4264	UI	P80
4730.9971	4730.9986	7207	0.2416	-1.4421	UI	P80
4731.5918	4731.5942	17437	0.1437	-2.3713	UII	P80
4732.5665	4732.5659	4412	0.3764	0.6569	UI	P80
4735.9068	4735.9008	415796	0.0274	6.0489	UI	RS21
4736.7728	4736.7725	17614	0.1362	0.2907	UI	P80
4737.6195	4737.6187	9658	0.1957	0.8417	UII	P80
4738.4391	4738.4384	34856	0.0930	0.6824	UI	P80
4739.1946	4739.1930	14935	0.1591	1.6088	UI	P80
4739.4993	4739.4993	3049	0.5341	0.0078	UI	P80
4741.7545	4741.7535	12482	0.1717	1.0582	UI	P80
4742.3307	4742.3307	31772	0.0998	-0.0811	UI	P80
4742.7943	4742.7921	3107	0.4675	2.2092	UI	P80
4743.5200	4743.5204	44938	0.0815	-0.4032	UI	P80
4744.0310	4744.0260	4746	0.3758	4.9194	UI	P80
4744.2966	4744.2965	12466	0.1657	0.1227	UII	P80

continued ...

Observed Wavelength Å	Ritz Wavelength Å	Relative Flux ADU	Uncertainty mÅ	Offset from Ritz wavelength mÅ	Species	Source
4748.3922	4748.3914	5875	0.2897	0.8046	UI	P80
4750.7130	4750.7175	4344	0.3817	-4.4830	UI	P80
4751.6583	4751.6618	7113	0.2370	-3.4020	UI	P80
4755.7356	4755.7363	17317	0.1384	-0.7126	UII	P80
4756.8053	4756.8054	219033	0.0370	-0.1351	UI	P80
4760.3392	4760.3446	2779	0.4884	-5.3193	UII	P80
4761.3300	4761.3298	8862	0.2079	0.2190	UI	P80
4762.8913	4762.8889	7290	0.2367	2.3204	UI	P80
4764.1500	4764.1484	4349	0.4180	1.5946	UII	P80
4768.6641	4768.6637	113925	0.0476	0.3623	UI	P80
4769.2665	4769.2662	23404	0.1211	0.2912	UII	P80
4771.7149	4771.7147	10379	0.1957	0.2248	UI	P80
4772.6956	4772.6945	31168	0.1073	1.0917	UII	P80
4773.4315	4773.4329	104394	0.0500	-1.3613	UI	P80
4774.3848	4774.3817	4005	0.4512	3.0762	UI	P80
4775.9223	4775.9213	5657	0.4185	1.0244	UI	P80
4777.6745	4777.6733	119239	0.0501	1.2509	UI	P80
4778.0949	4778.0961	22408	0.1347	-1.1658	UI	P80
4779.0913	4779.0927	5129	0.3465	-1.3959	UI	P80
4779.6317	4779.6291	17099	0.2051	2.5470	UII	P80
4780.1872	4780.1862	21764	0.1295	0.9705	UI	P80
4782.8051	4782.8108	12522	0.1935	-5.7330	UI	P80
4783.5015	4783.5072	3994	0.4228	-5.6984	UI	P80
4785.9177	4785.9194	31201	0.1115	-1.6376	UI	P80
4786.7260	4786.7294	4089	0.3843	-3.4876	UI	P80
4787.6089	4787.6030	3134	0.6331	5.9654	UI	P80
4790.3763	4790.3716	3452	0.4381	4.7015	UI	P80
4791.5687	4791.5739	3478	0.4229	-5.1459	UI	P80
4791.8286	4791.8349	4142	0.4089	-6.2967	UII	P80

continued ...

Observed Wavelength Å	Ritz Wavelength Å	Relative Flux ADU	Uncertainty mÅ	Offset from Ritz wavelength mÅ	Species	Source
4794.4869	4794.4805	3538	0.5030	6.4760	UI	P80
4799.7413	4799.7398	8699	0.2352	1.5290	UI	RS21
4800.2266	4800.2250	4824	0.3209	1.5695	UI	P80
4801.0522	4801.0571	5715	0.4715	-4.8595	UI	P80
4804.2333	4804.2290	4834	0.4550	4.3069	UI	P80
4807.6112	4807.6084	12321	0.1781	2.8065	UI	P80
4808.6012	4808.6007	3318	0.5473	0.5023	UI	P80
4808.8448	4808.8460	8837	0.2551	-1.2197	UI	P80
4809.9911	4809.9920	4124	0.4926	-0.9494	UI	P80
4810.8893	4810.8890	120712	0.0472	0.3542	UI	P80
4811.6877	4811.6890	15715	0.1651	-1.2715	UII	P80
4813.7838	4813.7819	3482	0.6101	1.9242	UI	P80
4814.0990	4814.1011	32126	0.1050	-2.1490	UI	P80
4815.7071	4815.7068	67231	0.0668	0.3002	UI	RS21
4818.6095	4818.6119	16843	0.1538	-2.3256	UI	P80
4819.2452	4819.2452	5825	0.3283	0.0366	UII	P80
4819.5438	4819.5492	14721	0.1670	-5.4271	UII	P80
4824.2771	4824.2816	11910	0.2225	-4.5213	UI	P80
4824.5019	4824.5031	5999	0.2968	-1.1386	UI	P80
4827.8425	4827.8432	2989	0.6156	-0.6981	UII	P80
4834.1768	4834.1798	5000	0.3169	-2.9531	UI	P80
4838.1805	4838.1794	3704	0.4297	1.1159	UI	P80
4841.0440	4841.0435	12916	0.1851	0.5421	UI	P80
4842.4838	4842.4884	170862	0.0490	-4.6124	UI	P80
4843.4944	4843.4892	10410	0.2012	5.2198	UII	P80
4844.7166	4844.7178	7816	0.2529	-1.2640	UII	P80
4845.6809	4845.6805	11721	0.1796	0.3814	UI	P80
4847.9991	4848.0006	43820	0.1164	-1.4772	UI	P80
4849.4004	4849.4001	3989	0.4170	0.3165	UII	RS21

continued ...

Observed Wavelength Å	Ritz Wavelength Å	Relative Flux ADU	Uncertainty mÅ	Offset from Ritz wavelength mÅ	Species	Source
4850.5979	4850.5968	4138	0.4426	1.0623	UI	RS21
4851.4593	4851.4565	6781	0.3130	2.7778	UI	P80
4852.1071	4852.1078	7690	0.2769	-0.6631	UII	P80
4852.9550	4852.9570	13745	0.1695	-1.9303	UI	P80
4854.8615	4854.8631	5751	0.3625	-1.5564	UI	P80
4856.0919	4856.0869	3017	0.6909	5.0034	UI	P80
4856.6559	4856.6564	15929	0.1541	-0.5167	UI	P80
4857.5041	4857.5017	4145	0.5324	2.4161	UII	P80
4858.0840	4858.0831	17122	0.1508	0.9350	UI	P80
4859.6933	4859.6919	18371	0.1442	1.4171	UII	P80
4860.9941	4860.9906	13506	0.1801	3.4586	UII	P80
4861.8263	4861.8240	10182	0.1999	2.3098	UI	P80
4863.4922	4863.4871	7166	0.2933	5.1486	UI	P80
4868.8633	4868.8582	34022	0.1021	5.1010	UI	P80
4869.0444	4869.0444	5326	0.3570	0.0065	UI	P80
4870.6423	4870.6447	6060	0.3011	-2.4100	UI	P80
4871.8002	4871.7944	8602	0.2190	5.7509	UI	P80
4874.0816	4874.0815	4514	0.3663	0.1196	UII	RS21
4874.3488	4874.3433	15053	0.1559	5.5596	UI	P80
4877.9915	4877.9866	4584	0.3864	4.9189	UII	P80
4878.5049	4878.5013	24168	0.1232	3.5856	UI	P80
4880.2544	4880.2549	12850	0.2640	-0.4221	UI	P80
4884.3477	4884.3460	5195	0.3558	1.6503	UI	P80
4885.1409	4885.1408	415284	0.0258	0.0324	UI	P80
4886.3307	4886.3249	9056	0.2885	5.7464	UII	P80
4886.6015	4886.6011	9494	0.2117	0.4140	UI	P80
4887.7332	4887.7308	6697	0.3347	2.3637	UI	P80
4891.1747	4891.1777	26232	0.1310	-3.0683	UI	P80
4892.6129	4892.6140	4727	0.4199	-1.1281	UII	P80

continued ...

Observed Wavelength Å	Ritz Wavelength Å	Relative Flux ADU	Uncertainty mÅ	Offset from Ritz wavelength mÅ	Species	Source
4894.7047	4894.7012	5006	0.4577	3.5187	UI	RS21
4895.6650	4895.6684	36415	0.1034	-3.3534	UI	P80
4896.0023	4896.0023	3448	0.5152	-0.0114	UI	P80
4898.6072	4898.6108	6888	0.3166	-3.6332	UII	P80
4899.2883	4899.2878	39554	0.1029	0.4726	UII	P80
4900.4353	4900.4338	3223	0.5324	1.5512	UII	RS21
4904.2057	4904.2050	5502	0.3099	0.7085	UI	P80
4906.2632	4906.2696	3100	0.4880	-6.4430	UI	P80
4909.3641	4909.3660	8114	0.2180	-1.9531	UI	P80
4910.3503	4910.3522	69760	0.0645	-1.9347	UI	P80
4911.6669	4911.6688	8951	0.2073	-1.8186	UII	P80
4913.1688	4913.1685	14620	0.1742	0.3291	UII	P80
4916.6356	4916.6358	18678	0.1563	-0.2001	UI	P80
4916.8718	4916.8739	17939	0.1540	-2.1011	UI	P80
4918.9042	4918.9019	6369	0.2917	2.2625	UI	P80
4919.1342	4919.1345	32311	0.1031	-0.2662	UI	P80
4920.1301	4920.1303	4665	0.3928	-0.1808	UI	P80
4921.3846	4921.3877	18004	0.1510	-3.1044	UI	P80
4923.6140	4923.6127	3430	0.5869	1.3311	UI	P80
4924.6423	4924.6444	11276	0.2102	-2.1895	UII	P80
4925.6604	4925.6614	3853	0.5335	-1.0338	UI	P80
4926.4405	4926.4389	6003	0.2852	1.5618	UII	P80
4927.6889	4927.6892	20660	0.1359	-0.2681	UI	P80
4928.1619	4928.1617	7520	0.2753	0.1622	UII	P80
4928.4490	4928.4474	223081	0.0370	1.5971	UI	P80
4933.6629	4933.6624	13641	0.1713	0.4416	UII	P80
4934.0274	4934.0315	4933	0.3975	-4.1010	UI	P80
4934.5624	4934.5609	4443	0.3700	1.5081	UI	P80
4936.9519	4936.9559	26522	0.1303	-3.9957	UII	P80

continued ...

Observed Wavelength Å	Ritz Wavelength Å	Relative Flux ADU	Uncertainty mÅ	Offset from Ritz wavelength mÅ	Species	Source
4937.9187	4937.9185	3438	0.7133	0.2508	UI	RS21
4938.9643	4938.9629	4169	0.4057	1.4280	UII	P80
4941.4692	4941.4676	8204	0.2491	1.6113	UI	P80
4942.6377	4942.6376	9699	0.2125	0.0503	UII	P80
4943.6909	4943.6921	5273	0.3146	-1.2189	UI	P80
4944.5022	4944.5045	89578	0.0592	-2.3173	UI	P80
4945.7639	4945.7639	4999	0.3282	-0.0145	UII	P80
4950.1702	4950.1715	5319	0.2959	-1.3441	UII	P80
4951.8427	4951.8467	4488	0.3655	-4.0437	UI	P80
4952.2203	4952.2199	2997	0.5480	0.3948	UI	P80
4954.9558	4954.9539	12668	0.1937	1.8475	UII	P80
4955.7741	4955.7752	43241	0.0972	-1.1779	UI	P80
4958.0666	4958.0689	9380	0.2120	-2.3251	UI	P80
4959.5334	4959.5356	14204	0.1764	-2.1723	UI	P80
4961.0966	4961.0959	3685	0.5884	0.6242	UII	P80
4961.5420	4961.5427	7182	0.2552	-0.7057	UI	P80
4963.3043	4963.3064	8827	0.2306	-2.1639	UI	P80
4967.3238	4967.3226	162544	0.0407	1.2319	UI	P80
4968.4444	4968.4408	4574	0.5249	3.5956	UI	P80
4969.0122	4969.0090	5032	0.4188	3.2406	UI	RS21
4970.2012	4970.2002	42467	0.0916	0.9832	UI	P80
4972.7239	4972.7237	9625	0.2230	0.2114	UI	P80
4981.9516	4981.9518	7747	0.2402	-0.1767	UI	P80
4984.6164	4984.6134	3092	0.4961	3.0411	UI	P80
4986.8923	4986.8974	9981	0.2367	-5.0700	UII	P80
4988.3311	4988.3320	5215	0.3054	-0.9092	UI	P80
4990.1145	4990.1173	11201	0.1841	-2.8547	UI	P80
4991.5951	4991.5977	3863	0.4237	-2.5509	UII	P80
4992.9279	4992.9304	4991	0.3239	-2.4674	UII	P80

continued ...

Observed Wavelength Å	Ritz Wavelength Å	Relative Flux ADU	Uncertainty mÅ	Offset from Ritz wavelength mÅ	Species	Source
4996.6205	4996.6215	3338	0.4613	-0.9354	UI	P80
4997.4107	4997.4128	7658	0.2444	-2.0758	UI	P80
4999.6072	4999.6123	4357	0.4591	-5.0482	UI	P80
4999.9463	4999.9429	5305	0.3449	3.3784	UII	P80
5001.5475	5001.5479	2996	0.5162	-0.3753	UI	P80
5004.0075	5004.0064	51668	0.0805	1.0744	UI	P80
5006.0135	5006.0105	6579	0.3159	3.0013	UI	P80
5008.2105	5008.2103	54933	0.0775	0.2571	UII	P80
5008.6844	5008.6798	37954	0.0974	4.6860	UI	P80
5011.4099	5011.4088	184751	0.0408	1.1143	UI	P80
5011.8287	5011.8263	7736	0.2996	2.3835	UI	P80
5012.4097	5012.4040	11135	0.2424	5.6640	UI	P80
5012.9231	5012.9268	5952	0.4155	-3.6798	UII	P80
5017.6373	5017.6400	4569	0.4682	-2.6552	UI	RS21
5021.1773	5021.1771	7474	0.2483	0.1858	UI	P80
5024.5669	5024.5673	12726	0.1824	-0.3536	UI	P80
5027.3835	5027.3837	741287	0.0202	-0.2543	UI	P80
5032.0403	5032.0435	3257	0.4129	-3.1843	UII	P80
5036.5227	5036.5255	8157	0.2433	-2.8623	UI	P80
5047.4038	5047.4038	9763	0.1992	0.0095	UII	P80
5048.8231	5048.8247	4707	0.4617	-1.6401	UII	RS21
5049.0484	5049.0473	35511	0.0924	1.0425	UI	P80
5051.4290	5051.4292	17403	0.1560	-0.1150	UI	P80
5052.6359	5052.6379	4387	0.4885	-1.9355	UI	P80
5053.3500	5053.3502	135836	0.0481	-0.1959	UI	P80
5054.1856	5054.1870	4091	0.5916	-1.3901	UI	RS21
5054.8039	5054.8074	3392	0.5362	-3.4804	UI	RS21
5055.4129	5055.4065	3321	0.5532	6.4248	UI	P80
5056.2144	5056.2165	5737	0.3092	-2.0922	UI	P80

continued ...

Observed Wavelength Å	Ritz Wavelength Å	Relative Flux ADU	Uncertainty mÅ	Offset from Ritz wavelength mÅ	Species	Source
5057.1762	5057.1777	6150	0.2983	-1.4680	UI	P80
5059.2402	5059.2401	2636	0.5549	0.1294	UI	P80
5059.5556	5059.5522	3329	0.5119	3.4019	UI	P80
5061.4891	5061.4874	5684	0.3300	1.7233	UI	P80
5062.0371	5062.0390	140353	0.0494	-1.9228	UI	RS21
5063.7575	5063.7582	60081	0.0760	-0.7348	UI	P80
5067.2110	5067.2122	3152	0.4742	-1.2463	UI	P80
5074.7636	5074.7636	11995	0.1819	-0.0012	UI	P80
5076.7502	5076.7508	28298	0.1060	-0.6011	UI	P80
5076.9867	5076.9870	5458	0.2968	-0.2872	UI	P80
5077.8059	5077.8054	7354	0.2376	0.4715	UI	P80
5078.1978	5078.1979	4140	0.3650	-0.1034	UI	P80
5080.4818	5080.4802	9721	0.2239	1.6068	UI	P80
5081.4042	5081.3976	6657	0.2893	6.5324	UI	P80
5086.8147	5086.8142	3481	0.4875	0.5209	UI	P80
5088.2859	5088.2857	142938	0.0471	0.1395	UI	P80
5090.1543	5090.1549	3497	0.5078	-0.6212	UI	P80
5090.4964	5090.4961	46358	0.0939	0.3236	UI	RS21
5091.2878	5091.2865	3575	0.5564	1.2642	UI	RS21
5093.0986	5093.0956	39521	0.1008	3.0077	UI	P80
5093.8939	5093.8934	8550	0.2665	0.4979	UI	P80
5101.0074	5101.0076	42458	0.0886	-0.1498	UI	P80
5101.7427	5101.7428	5999	0.3071	-0.0397	UI	P80
5106.7384	5106.7330	10204	0.2157	5.4510	UI	P80
5107.3229	5107.3261	5610	0.3500	-3.2210	UI	P80
5107.6756	5107.6768	27706	0.1141	-1.1812	UI	P80
5109.3855	5109.3832	3785	0.4383	2.2577	UI	P80
5110.6864	5110.6857	10815	0.1986	0.6939	UI	P80
5115.8251	5115.8274	4114	0.3933	-2.3081	UI	P80

continued ...

Observed Wavelength Å	Ritz Wavelength Å	Relative Flux ADU	Uncertainty mÅ	Offset from Ritz wavelength mÅ	Species	Source
5116.9251	5116.9270	3696	0.4464	-1.8851	UI	P80
5117.2393	5117.2380	17791	0.1497	1.2739	UII	P80
5119.5017	5119.5018	23281	0.1244	-0.0568	UI	P80
5120.4184	5120.4211	4376	0.3749	-2.6555	UI	P80
5123.3301	5123.3327	2901	0.5948	-2.6519	UII	P80
5124.0816	5124.0821	16928	0.1475	-0.4612	UI	P80
5124.9427	5124.9430	7897	0.2531	-0.2506	UI	P80
5125.4846	5125.4911	16191	0.1703	-6.4349	UI	P80
5126.1468	5126.1481	5702	0.4352	-1.3276	UII	P80
5128.3598	5128.3602	15725	0.1644	-0.3560	UI	P80
5130.1546	5130.1597	5219	0.3958	-5.0816	UI	P80
5132.1908	5132.1905	32363	0.1041	0.3270	UI	P80
5132.6183	5132.6146	5609	0.3775	3.7370	UI	P80
5134.1866	5134.1858	16095	0.1805	0.7730	UI	P80
5136.5188	5136.5224	3979	0.7911	-3.5516	UI	RS21
5137.0460	5137.0462	11284	0.2561	-0.1230	UII	P80
5139.3401	5139.3404	10841	0.2774	-0.2600	UI	P80
5139.9772	5139.9788	19641	0.1936	-1.5795	UII	P80
5140.4089	5140.4083	6054	0.4297	0.6401	UII	RS21
5141.7827	5141.7819	193113	0.0437	0.8210	UII	RS21
5142.3946	5142.3945	44154	0.0912	0.0809	UI	P80
5142.7167	5142.7164	11417	0.2327	0.3452	UI	P80
5144.5141	5144.5146	42692	0.0946	-0.5644	UI	P80
5146.9849	5146.9858	25294	0.1231	-0.9331	UI	P80
5147.9432	5147.9388	3213	0.6538	4.3544	UI	P80
5148.9574	5148.9590	6567	0.3050	-1.6019	UI	P80
5149.2433	5149.2434	8261	0.2533	-0.0968	UI	P80
5151.3903	5151.3935	12346	0.2043	-3.2236	UI	RS21
5152.1313	5152.1309	3442	0.5719	0.3722	UI	P80

continued ...

Observed Wavelength Å	Ritz Wavelength Å	Relative Flux ADU	Uncertainty mÅ	Offset from Ritz wavelength mÅ	Species	Source
5152.3868	5152.3871	6759	0.3973	-0.3113	UI	P80
5152.7733	5152.7709	4576	0.5028	2.3861	UI	P80
5153.3901	5153.3914	3096	0.6225	-1.2950	UI	P80
5154.2147	5154.2186	12571	0.2069	-3.8807	UI	P80
5156.0262	5156.0327	10281	0.2565	-6.4586	UI	P80
5156.5591	5156.5599	3428	0.4976	-0.7452	UI	P80
5160.3178	5160.3159	22493	0.1322	1.8417	UI	P80
5160.6675	5160.6676	11026	0.2014	-0.1101	UI	P80
5164.1378	5164.1384	58676	0.0743	-0.5563	UI	P80
5166.7362	5166.7422	3840	0.5646	-5.9842	UI	P80
5168.4074	5168.4023	4827	0.3852	5.1234	UI	P80
5170.8925	5170.8918	4729	0.3712	0.6970	UI	P80
5171.6401	5171.6452	4150	0.5988	-5.1121	UI	P80
5172.6563	5172.6549	4798	0.4076	1.3604	UI	P80
5174.3188	5174.3188	14021	0.1767	0.0163	UI	P80
5174.9826	5174.9837	3407	0.6151	-1.1465	UI	RS21
5175.6828	5175.6776	4230	0.4840	5.2509	UI	P80
5177.2103	5177.2146	5567	0.4176	-4.2612	UI	P80
5178.1126	5178.1154	4290	0.6034	-2.8481	UI	RS21
5180.0136	5180.0124	7452	0.3288	1.2133	UI	P80
5180.6677	5180.6662	64645	0.0773	1.4746	UI	P80
5180.8776	5180.8786	96991	0.0618	-0.9994	UI	P80
5183.0274	5183.0253	9083	0.2839	2.1249	UI	P80
5184.2180	5184.2233	4681	0.5912	-5.2535	UI	RS21
5184.5751	5184.5719	31851	0.1291	3.1926	UI	P80
5188.5589	5188.5609	13622	0.2018	-2.0175	UI	P80
5189.2000	5189.2026	9197	0.2522	-2.6137	UI	P80
5189.8668	5189.8709	3378	0.6385	-4.0841	UI	RS21
5191.5098	5191.5121	55844	0.0906	-2.3187	UI	P80

continued ...

Observed Wavelength Å	Ritz Wavelength Å	Relative Flux ADU	Uncertainty mÅ	Offset from Ritz wavelength mÅ	Species	Source
5192.0030	5192.0019	16324	0.1707	1.1256	UI	P80
5193.8911	5193.8954	4989	0.3994	-4.2291	UI	P80
5196.4590	5196.4570	3796	0.5208	2.0545	UI	P80
5197.9876	5197.9863	3156	0.6191	1.2783	UII	P80
5201.4644	5201.4641	4968	0.3790	0.2515	UI	P80
5202.4539	5202.4533	4002	0.4530	0.6015	UII	P80
5205.1595	5205.1620	111618	0.0571	-2.5651	UI	P80
5206.0028	5206.0059	7051	0.2830	-3.1172	UI	P80
5207.7850	5207.7862	19293	0.1445	-1.1927	UI	P80
5212.4848	5212.4882	3245	0.5487	-3.3841	UI	P80
5212.7334	5212.7323	4898	0.3691	1.0915	UI	P80
5215.1782	5215.1792	25604	0.1263	-0.9908	UI	P80
5216.1638	5216.1651	3330	0.7314	-1.2999	UI	P80
5216.9317	5216.9333	130834	0.0536	-1.5644	UI	P80
5218.5501	5218.5476	9908	0.2351	2.5532	UI	P80
5221.8929	5221.8963	106018	0.0602	-3.4228	UI	P80
5223.7827	5223.7845	4728	0.6170	-1.7867	UI	P80
5224.2804	5224.2825	8475	0.2916	-2.1212	UII	P80
5225.1195	5225.1209	17538	0.1744	-1.4194	UII	P80
5226.4857	5226.4873	13142	0.2044	-1.5726	UI	P80
5228.7342	5228.7328	5820	0.5060	1.3424	UII	P80
5228.9971	5228.9967	8676	0.3424	0.4153	UI	P80
5229.2913	5229.2927	26224	0.1232	-1.3998	UI	P80
5230.2933	5230.2951	7698	0.3126	-1.7669	UI	P80
5230.9984	5230.9991	8359	0.2770	-0.6561	UI	P80
5232.1654	5232.1685	17149	0.1820	-3.0790	UI	P80
5232.8012	5232.8029	32601	0.1164	-1.6436	UI	P80
5233.2089	5233.2084	7100	0.3120	0.4633	UI	P80
5234.1586	5234.1594	36685	0.1025	-0.8172	UI	P80

continued ...

Observed Wavelength Å	Ritz Wavelength Å	Relative Flux ADU	Uncertainty mÅ	Offset from Ritz wavelength mÅ	Species	Source
5238.6174	5238.6159	5479	0.3498	1.5511	UII	P80
5239.3574	5239.3580	25056	0.1251	-0.6145	UI	P80
5240.0093	5240.0113	5715	0.3283	-1.9850	UI	P80
5241.7828	5241.7837	37305	0.0971	-0.9522	UI	P80
5242.3049	5242.3007	5587	0.3757	4.1549	UI	P80
5243.4963	5243.4951	3211	0.5438	1.2482	UI	P80
5244.6840	5244.6835	10223	0.2299	0.4275	UI	P80
5247.3525	5247.3525	7462	0.2624	-0.0360	UII	P80
5247.7407	5247.7410	18696	0.1959	-0.3054	UI	P80
5248.0212	5248.0256	8562	0.2573	-4.3629	UI	P80
5250.7412	5250.7416	4587	0.3914	-0.4117	UI	P80
5251.2098	5251.2081	7232	0.2995	1.7072	UI	P80
5253.5597	5253.5580	3122	0.5438	1.6365	UI	P80
5253.8656	5253.8687	7470	0.2800	-3.0712	UI	P80
5255.2754	5255.2706	8806	0.2631	4.7322	UI	P80
5255.6920	5255.6910	6110	0.3279	1.0269	UI	P80
5257.0477	5257.0448	15288	0.2005	2.9279	UII	P80
5258.7188	5258.7180	5869	0.3404	0.7581	UI	P80
5259.9040	5259.9031	22366	0.1319	0.8862	UI	P80
5263.4238	5263.4232	5298	0.4211	0.5865	UII	RS21
5263.8651	5263.8665	7561	0.2876	-1.3827	UI	P80
5265.9885	5265.9915	4818	0.5218	-3.0075	UI	P80
5268.5516	5268.5510	20971	0.1543	0.5882	UI	P80
5270.1818	5270.1860	4936	0.5146	-4.2466	UII	P80
5270.4318	5270.4291	8502	0.3756	2.6412	UII	P80
5270.6281	5270.6289	56643	0.0833	-0.7135	UI	P80
5272.0058	5272.0050	51709	0.0949	0.8151	UI	P80
5273.2402	5273.2418	7601	0.3131	-1.5573	UI	P80
5275.1975	5275.1928	6233	0.3401	4.6702	UI	P80

continued ...

Observed Wavelength Å	Ritz Wavelength Å	Relative Flux ADU	Uncertainty mÅ	Offset from Ritz wavelength mÅ	Species	Source
5275.9246	5275.9258	45571	0.0936	-1.2047	UI	P80
5278.1699	5278.1683	10023	0.2548	1.5700	UII	P80
5280.3798	5280.3790	495695	0.0269	0.7330	UI	P80
5283.3812	5283.3757	6134	0.4682	5.5051	UI	P80
5283.5768	5283.5780	32953	0.1121	-1.2444	UI	P80
5286.0838	5286.0875	3968	0.4570	-3.6860	UII	P80
5288.3786	5288.3797	4950	0.3629	-1.1233	UII	P80
5294.0306	5294.0310	7093	0.2863	-0.3549	UI	P80
5297.4452	5297.4461	36797	0.1009	-0.9267	UI	P80
5299.4415	5299.4404	5421	0.3748	1.1214	UI	P80
5300.5706	5300.5687	23733	0.1274	1.8935	UI	P80
5303.0979	5303.0927	12242	0.2035	5.2849	UI	P80
5304.5676	5304.5700	4789	0.4444	-2.3196	UI	P80
5306.5896	5306.5872	12491	0.1885	2.4619	UI	P80
5308.5420	5308.5409	253604	0.0363	1.0784	UI	P80
5310.0426	5310.0438	15808	0.1623	-1.2496	UI	P80
5310.4779	5310.4752	4555	0.3951	2.6745	UII	P80
5310.6818	5310.6780	5649	0.3543	3.7814	UI	P80
5313.2559	5313.2546	5583	0.4170	1.2409	UII	RS21
5315.2759	5315.2779	49517	0.0936	-1.9884	UI	P80
5319.0104	5319.0079	5321	0.4157	2.5267	UI	P80
5319.3901	5319.3959	11292	0.2375	-5.8164	UI	P80
5320.4431	5320.4432	10732	0.2322	-0.0974	UI	P80
5321.6066	5321.6048	6784	0.3183	1.7777	UII	P80
5322.7867	5322.7830	33173	0.1146	3.6621	UII	P80
5325.4991	5325.5027	4821	0.4173	-3.5862	UI	P80
5327.3261	5327.3246	6649	0.3822	1.4330	UII	P80
5327.7543	5327.7555	7330	0.2871	-1.1480	UII	P80
5329.2620	5329.2648	66773	0.0779	-2.8696	UII	P80

continued ...

Observed Wavelength Å	Ritz Wavelength Å	Relative Flux ADU	Uncertainty mÅ	Offset from Ritz wavelength mÅ	Species	Source
5331.5731	5331.5774	3347	0.5376	-4.3604	UI	P80
5336.5423	5336.5436	19552	0.1438	-1.2244	UI	P80
5341.5078	5341.5056	28416	0.1117	2.2144	UI	P80
5344.2761	5344.2735	2800	0.6729	2.6315	UI	P80
5345.3359	5345.3372	4480	0.3900	-1.3089	UI	P80
5346.6421	5346.6404	5952	0.3216	1.6968	UI	P80
5348.9878	5348.9922	4419	0.4025	-4.3258	UI	P80
5354.3596	5354.3588	6371	0.3043	0.8249	UI	P80
5355.3694	5355.3716	6263	0.3310	-2.2649	UI	P80
5355.5783	5355.5767	10725	0.2088	1.5550	UI	RS21
5356.5736	5356.5749	11254	0.2114	-1.3310	UII	P80
5357.1871	5357.1854	3833	0.5531	1.7009	UI	RS21
5359.0469	5359.0526	4057	0.9030	-5.7327	UII	RS21
5359.4233	5359.4264	8050	0.3056	-3.0304	UI	P80
5363.8033	5363.8054	10024	0.2534	-2.0909	UII	P80
5364.0616	5364.0622	5620	0.5112	-0.6519	UII	P80
5364.7135	5364.7122	16075	0.1838	1.3876	UI	P80
5368.3860	5368.3835	12973	0.2401	2.4710	UI	P80
5370.9126	5370.9162	4818	0.4547	-3.5637	UI	P80
5371.3491	5371.3513	4583	0.4103	-2.1899	UI	P80
5373.9965	5373.9933	4178	0.5364	3.1218	UII	RS21
5374.2129	5374.2134	3534	0.6321	-0.5190	UI	P80
5375.5009	5375.5008	14406	0.1759	0.1026	UI	P80
5375.7595	5375.7616	13423	0.1824	-2.1186	UI	P80
5378.1085	5378.1125	6759	0.3261	-4.0331	UI	P80
5378.6836	5378.6827	2850	0.5902	0.8372	UI	P80
5382.0047	5382.0020	6514	0.5688	2.7435	UI	P80
5382.9289	5382.9302	45027	0.0940	-1.3296	UI	P80
5386.1982	5386.1924	5040	0.4121	5.8655	UII	P80

continued ...

Observed Wavelength Å	Ritz Wavelength Å	Relative Flux ADU	Uncertainty mÅ	Offset from Ritz wavelength mÅ	Species	Source
5390.2789	5390.2780	4543	0.4592	0.8385	UI	P80
5391.0932	5391.0910	3874	0.4619	2.1341	UI	P80
5392.8303	5392.8348	4275	0.4485	-4.5073	UII	RS21
5394.4708	5394.4745	2975	0.5898	-3.6532	UI	P80
5395.5421	5395.5418	7448	0.2788	0.2191	UI	P80
5398.8372	5398.8392	4252	0.4779	-2.0465	UI	RS21
5399.5302	5399.5289	9291	0.2711	1.3243	UII	P80
5400.9161	5400.9100	21086	0.1666	6.0956	UI	P80
5401.4229	5401.4223	3097	0.6266	0.5008	UI	P80
5401.8918	5401.8915	13729	0.1781	0.3218	UI	P80
5403.1834	5403.1876	9523	0.2342	-4.1815	UII	P80
5404.6629	5404.6573	5946	0.4886	5.5972	UI	RS21
5405.9760	5405.9736	11086	0.2370	2.4018	UII	P80
5406.3760	5406.3802	13942	0.2518	-4.1619	UI	P80
5406.6318	5406.6326	7004	0.4066	-0.8053	UI	RS21
5406.8689	5406.8690	33959	0.1176	-0.1576	UI	P80
5407.8207	5407.8230	5733	0.4691	-2.2742	UI	P80
5408.1336	5408.1338	4407	0.6040	-0.2426	UII	RS21
5408.3290	5408.3224	4441	0.5766	6.5461	UI	RS21
5409.0787	5409.0757	6034	0.4003	3.0448	UII	P80
5410.2337	5410.2334	42285	0.0994	0.2281	UI	P80
5414.7546	5414.7578	12045	0.2231	-3.2072	UI	P80
5416.5641	5416.5616	3239	0.7865	2.4898	UI	RS21
5419.3699	5419.3717	4510	0.4244	-1.7559	UI	P80
5423.3519	5423.3567	15547	0.1727	-4.8080	UI	P80
5424.7042	5424.7023	3101	0.5690	1.8820	UII	P80
5426.6751	5426.6779	5421	0.3359	-2.7803	UI	P80
5429.0462	5429.0458	4593	0.4009	0.3338	UI	P80
5430.2346	5430.2358	10791	0.2103	-1.1626	UI	P80

continued ...

Observed Wavelength Å	Ritz Wavelength Å	Relative Flux ADU	Uncertainty mÅ	Offset from Ritz wavelength mÅ	Species	Source
5431.3469	5431.3473	22550	0.1352	-0.3971	UI	P80
5438.6276	5438.6292	3352	0.5489	-1.5227	UI	P80
5439.0831	5439.0863	3132	0.5034	-3.2317	UI	P80
5441.0803	5441.0839	3540	0.5894	-3.6148	UI	P80
5441.9921	5441.9910	3393	0.6400	1.0631	UI	P80
5443.9400	5443.9404	4546	0.4524	-0.3841	UI	P80
5444.4685	5444.4685	6666	0.3158	0.0243	UI	P80
5445.8674	5445.8657	6554	0.2945	1.7554	UI	P80
5447.0558	5447.0508	4403	0.5080	4.9027	UI	P80
5451.6585	5451.6561	33215	0.1159	2.3742	UII	RS21
5452.3952	5452.3937	17897	0.1763	1.5691	UI	P80
5453.4219	5453.4213	5343	0.4938	0.6585	UII	RS21
5455.2466	5455.2481	4175	0.6547	-1.4308	UI	P80
5455.5884	5455.5888	8743	0.2897	-0.3505	UII	P80
5456.1289	5456.1285	6579	0.4226	0.4130	UI	P80
5456.7770	5456.7729	8038	0.3278	4.0557	UI	P80
5459.2512	5459.2505	59872	0.0939	0.6318	UI	P80
5459.5678	5459.5673	9623	0.3171	0.4560	UI	P80
5461.2912	5461.2875	3577	0.6977	3.7082	UI	P80
5464.2235	5464.2235	50277	0.0924	-0.0127	UI	P80
5475.7091	5475.7059	11153	0.2442	3.1836	UII	P80
5476.2905	5476.2877	2750	0.5973	2.7920	UI	P80
5476.7637	5476.7687	5957	0.3297	-4.9937	UI	P80
5477.4996	5477.5019	3231	0.5604	-2.3056	UII	P80
5477.8460	5477.8478	12792	0.1883	-1.7562	UI	P80
5480.2628	5480.2618	6901	0.3308	0.9445	UII	P80
5487.0020	5487.0019	7522	0.2804	0.0420	UII	RS21
5487.2396	5487.2390	3290	0.6197	0.5814	UI	P80
5488.8837	5488.8831	8970	0.2370	0.6517	UI	P80

continued ...

Observed Wavelength Å	Ritz Wavelength Å	Relative Flux ADU	Uncertainty mÅ	Offset from Ritz wavelength mÅ	Species	Source
5491.2211	5491.2197	5551	0.4012	1.4420	UII	P80
5492.9504	5492.9510	126206	0.0530	-0.5884	UII	P80
5494.6042	5494.6103	13587	0.2542	-6.0482	UI	P80
5495.2984	5495.2981	19984	0.1479	0.2694	UI	P80
5496.4267	5496.4264	107653	0.0571	0.3598	UI	P80
5497.7437	5497.7429	12744	0.1936	0.8380	UI	P80
5498.1776	5498.1764	9692	0.2478	1.2035	UI	RS21
5498.9745	5498.9726	3833	0.5104	1.9110	UI	P80
5500.1015	5500.1000	3285	0.5898	1.4793	UI	P80
5500.6838	5500.6840	178079	0.0459	-0.1772	UI	P80
5501.4927	5501.4928	8892	0.3446	-0.1465	UII	P80
5501.8137	5501.8157	28807	0.1292	-1.9245	UI	P80
5502.1844	5502.1853	49082	0.0954	-0.9329	UI	P80
5503.6479	5503.6513	3687	0.6815	-3.3961	UI	RS21
5504.1254	5504.1218	18440	0.1734	3.5104	UI	P80
5505.4724	5505.4705	6736	0.3782	1.9583	UI	P80
5507.0590	5507.0567	4114	0.7125	2.2226	UI	P80
5509.3066	5509.3092	3818	0.6381	-2.6390	UI	RS21
5510.1175	5510.1193	6124	0.4441	-1.8921	UI	P80
5510.4146	5510.4159	29400	0.1273	-1.3607	UI	P80
5511.0858	5511.0799	6226	0.4880	5.9899	UII	RS21
5511.4948	5511.4958	677221	0.0225	-1.0340	UI	P80
5513.8311	5513.8303	4520	0.5338	0.7812	UI	RS21
5515.1163	5515.1160	5971	0.3663	0.2807	UI	P80
5518.1395	5518.1417	3052	0.5763	-2.2066	UI	P80
5519.3330	5519.3330	3061	0.6931	0.0277	UI	RS21
5519.8072	5519.8085	3670	0.5426	-1.3760	UI	P80
5521.0242	5521.0267	26719	0.1259	-2.4835	UI	P80
5522.9248	5522.9247	3025	0.5639	0.1642	UI	P80

continued ...

Observed Wavelength Å	Ritz Wavelength Å	Relative Flux ADU	Uncertainty mÅ	Offset from Ritz wavelength mÅ	Species	Source
5524.9611	5524.9599	5793	0.3537	1.1334	UI	RS21
5526.3317	5526.3343	8755	0.2486	-2.6300	UI	P80
5527.9759	5527.9810	34784	0.1236	-5.0314	UII	P80
5530.6983	5530.6976	4969	0.3794	0.7346	UI	P80
5531.2693	5531.2719	19686	0.1732	-2.6361	UI	P80
5533.0862	5533.0896	3208	0.4971	-3.4284	UI	P80
5534.7137	5534.7182	14014	0.1994	-4.4409	UI	P80
5535.7755	5535.7765	4641	0.3915	-1.0298	UII	P80
5536.5289	5536.5262	3113	0.5677	2.6879	UI	P80
5538.1910	5538.1867	3002	0.6555	4.2582	UI	P80
5542.8936	5542.8958	2788	0.6199	-2.2918	UI	RS21
5545.0521	5545.0504	4743	0.4769	1.7297	UI	RS21
5545.7478	5545.7497	5063	0.4441	-1.8808	UI	P80
5546.0958	5546.0934	3011	0.6772	2.3524	UII	RS21
5548.0388	5548.0399	4198	0.4772	-1.0815	UII	P80
5551.4200	5551.4240	11811	0.2539	-4.0203	UII	P80
5553.6859	5553.6864	9097	0.2992	-0.5305	UI	P80
5557.8806	5557.8806	165726	0.0479	0.0001	UI	P80
5558.7048	5558.7020	149089	0.0541	2.7652	UI	RS21
5559.8818	5559.8837	20981	0.2148	-1.9089	UI	P80
5562.4633	5562.4643	5445	0.4651	-0.9141	UI	P80
5563.7963	5563.7981	60387	0.0928	-1.7912	UI	P80
5564.1708	5564.1707	696105	0.0229	0.1085	UI	P80
5564.6219	5564.6171	7917	0.4107	4.8110	UI	P80
5568.4876	5568.4867	16871	0.1674	0.9774	UI	P80
5570.6622	5570.6636	10042	0.2422	-1.3493	UII	P80
5573.0719	5573.0739	10728	0.2282	-2.0126	UI	P80
5573.5904	5573.5910	24687	0.1334	-0.6050	UI	P80
5574.6538	5574.6533	16352	0.1697	0.5084	UI	P80

continued ...

Observed Wavelength Å	Ritz Wavelength Å	Relative Flux ADU	Uncertainty mÅ	Offset from Ritz wavelength mÅ	Species	Source
5577.0366	5577.0379	5108	0.4173	-1.3480	UI	P80
5577.6823	5577.6791	10808	0.2792	3.1995	UII	RS21
5578.5169	5578.5222	4778	0.5242	-5.3268	UI	RS21
5580.8031	5580.8055	5139	0.3638	-2.3901	UII	P80
5581.2222	5581.2236	11485	0.2050	-1.4498	UII	P80
5581.6013	5581.6034	25330	0.1395	-2.0692	UII	P80
5584.6218	5584.6209	12948	0.1860	0.8789	UI	P80
5589.3714	5589.3727	2770	0.5926	-1.3269	UI	P80
5591.1024	5591.1018	7119	0.2885	0.5849	UI	P80
5591.7083	5591.7126	3909	0.5714	-4.2488	UI	P80
5595.1411	5595.1429	3787	0.4774	-1.7908	UI	P80
5596.2816	5596.2856	5523	0.4163	-3.9788	UI	P80
5603.0550	5603.0555	13252	0.2674	-0.4724	UI	P80
5603.9685	5603.9732	10454	0.2721	-4.7288	UII	P80
5608.8446	5608.8484	14181	0.2677	-3.7276	UI	P80
5609.2941	5609.2965	11335	0.2633	-2.3102	UI	P80
5610.2450	5610.2402	4529	0.6141	4.8120	UI	RS21
5610.8900	5610.8903	266537	0.0376	-0.2907	UI	P80
5612.3158	5612.3120	9612	0.3355	3.8265	UII	P80
5613.2602	5613.2623	24238	0.1500	-2.1195	UI	P80
5614.7450	5614.7438	16600	0.2042	1.1659	UI	P80
5616.5747	5616.5736	45517	0.0998	1.0803	UI	P80
5616.8800	5616.8775	14058	0.2349	2.5516	UII	P80
5618.5058	5618.5046	6324	0.3325	1.1989	UI	P80
5620.7795	5620.7763	608192	0.0241	3.1995	UI	P80
5621.5177	5621.5134	129132	0.0549	4.3428	UI	P80
5622.5512	5622.5477	19058	0.1662	3.4662	UI	P80
5622.9783	5622.9844	5010	0.4038	-6.0424	UI	P80
5624.6118	5624.6082	3873	0.6276	3.5898	UI	P80

continued ...

Observed Wavelength Å	Ritz Wavelength Å	Relative Flux ADU	Uncertainty mÅ	Offset from Ritz wavelength mÅ	Species	Source
5625.0088	5625.0038	11857	0.2374	4.9774	UI	P80
5628.1508	5628.1557	29614	0.1331	-4.9345	UI	P80
5628.9857	5628.9876	5589	0.3796	-1.8730	UI	P80
5641.6665	5641.6605	3852	0.6114	6.0070	UI	P80
5642.5914	5642.5896	4192	0.5664	1.7556	UI	P80
5645.9397	5645.9381	12208	0.2134	1.5889	UI	P80
5646.7460	5646.7447	5495	0.4247	1.2581	UI	P80
5653.3290	5653.3276	9473	0.3249	1.4004	UI	P80
5653.7703	5653.7703	14460	0.2302	0.0080	UII	P80
5654.8022	5654.8022	93105	0.0681	-0.0123	UI	P80
5655.4022	5655.4007	10919	0.3186	1.4214	UI	P80
5655.6046	5655.6076	22474	0.1670	-3.0286	UI	P80
5656.7919	5656.7889	5251	0.5676	2.9542	UI	P80
5657.5113	5657.5104	16467	0.2203	0.8701	UI	P80
5657.7365	5657.7406	9139	0.3481	-4.1102	UI	P80
5658.2680	5658.2634	110159	0.0672	4.6127	UI	P80
5658.8226	5658.8239	4928	0.6396	-1.3430	UII	RS21
5659.7085	5659.7099	10742	0.2901	-1.4730	UI	P80
5662.0505	5662.0483	6525	0.4706	2.1610	UI	P80
5663.0780	5663.0763	12984	0.2343	1.6974	UI	P80
5664.2295	5664.2288	11383	0.3265	0.7534	UII	P80
5665.7949	5665.7918	15260	0.2138	3.0951	UI	P80
5668.7308	5668.7347	5200	0.5131	-3.9373	UI	P80
5671.2478	5671.2496	3240	0.6541	-1.7787	UI	P80
5674.2533	5674.2541	9330	0.2558	-0.8798	UII	P80
5676.1255	5676.1249	6405	0.3454	0.6691	UI	P80
5680.3703	5680.3724	14482	0.2061	-2.1359	UI	P80
5682.4445	5682.4465	5374	0.3957	-2.0215	UI	P80
5685.2097	5685.2110	40070	0.1047	-1.3137	UI	P80

continued ...

Observed Wavelength Å	Ritz Wavelength Å	Relative Flux ADU	Uncertainty mÅ	Offset from Ritz wavelength mÅ	Species	Source
5686.4546	5686.4540	3853	0.5228	0.6656	UI	P80
5688.3405	5688.3448	2853	0.6314	-4.3074	UI	P80
5691.3440	5691.3415	75663	0.0801	2.5137	UI	P80
5692.1695	5692.1732	4115	0.4662	-3.6204	UI	P80
5694.8454	5694.8419	9171	0.2892	3.4813	UI	P80
5695.1802	5695.1816	18523	0.1615	-1.3369	UI	P80
5696.0820	5696.0841	3320	0.6400	-2.1060	UI	P80
5697.5225	5697.5233	3969	0.4947	-0.8659	UI	P80
5698.3264	5698.3320	4831	0.4675	-5.6284	UI	RS21
5699.2573	5699.2540	7149	0.3552	3.3760	UI	P80
5699.8742	5699.8746	57429	0.0832	-0.4481	UI	P80
5702.2546	5702.2571	4617	0.6129	-2.5136	UI	P80
5702.8506	5702.8505	32181	0.1136	0.1277	UI	P80
5704.6312	5704.6353	5869	0.5355	-4.0017	UI	P80
5705.3309	5705.3296	10312	0.3054	1.3288	UI	P80
5706.6846	5706.6851	41477	0.1113	-0.5366	UI	P80
5706.9964	5706.9924	9415	0.3141	3.9400	UI	P80
5707.2978	5707.2979	14231	0.2240	-0.0929	UI	P80
5708.2186	5708.2233	4295	0.8278	-4.7090	UI	RS21
5709.4936	5709.4930	47747	0.1010	0.6786	UI	P80
5714.2083	5714.2091	37273	0.1166	-0.7544	UI	P80
5715.2272	5715.2280	51121	0.0942	-0.8134	UI	P80
5715.6977	5715.6983	77775	0.0739	-0.6899	UI	P80
5716.8745	5716.8749	133189	0.0546	-0.4332	UI	P80
5717.2767	5717.2804	7408	0.3617	-3.6372	UI	P80
5719.5001	5719.4978	6243	0.4460	2.2293	UI	P80
5721.5800	5721.5757	25183	0.1598	4.3412	UI	P80
5722.2367	5722.2371	21122	0.1811	-0.3836	UI	P80
5726.3134	5726.3111	6117	0.3513	2.2735	UI	P80

continued ...

Observed Wavelength Å	Ritz Wavelength Å	Relative Flux ADU	Uncertainty mÅ	Offset from Ritz wavelength mÅ	Species	Source
5728.9321	5728.9338	9437	0.2506	-1.6366	UI	P80
5730.0174	5730.0163	3273	0.5890	1.1052	UII	P80
5730.8932	5730.8978	3488	0.5592	-4.6644	UI	P80
5731.4838	5731.4824	7178	0.3387	1.3254	UI	P80
5731.8675	5731.8688	20775	0.1479	-1.3235	UI	P80
5732.7283	5732.7290	9062	0.2704	-0.7070	UI	P80
5734.3522	5734.3558	3615	0.5184	-3.6108	UI	P80
5736.3903	5736.3918	32809	0.1193	-1.4681	UI	P80
5737.2767	5737.2727	25614	0.1466	4.0772	UI	P80
5741.3205	5741.3211	22396	0.1394	-0.6241	UI	P80
5742.7723	5742.7673	6102	0.3407	5.0350	UI	RS21
5748.1032	5748.1033	7406	0.3009	-0.0885	UII	P80
5748.4463	5748.4493	4561	0.4725	-2.9566	UII	P80
5748.7829	5748.7850	3556	0.5397	-2.1032	UII	RS21
5750.5500	5750.5547	15578	0.1856	-4.7107	UI	P80
5751.7374	5751.7366	37556	0.1075	0.8026	UI	P80
5755.1570	5755.1590	9598	0.2409	-1.9398	UI	P80
5755.6042	5755.6055	10528	0.2215	-1.3304	UI	P80
5756.8714	5756.8736	3063	0.6512	-2.2582	UI	P80
5757.3128	5757.3140	34633	0.1125	-1.1609	UI	P80
5758.1426	5758.1430	302605	0.0382	-0.3953	UI	P80
5758.3548	5758.3568	120921	0.0678	-1.9979	UI	P80
5761.2679	5761.2650	3620	0.9269	2.8855	UII	RS21
5762.8526	5762.8496	4062	0.7816	2.9448	UI	RS21
5765.3829	5765.3799	19008	0.1855	3.0445	UI	P80
5767.4466	5767.4437	34882	0.1244	2.8334	UII	P80
5767.6965	5767.6959	6070	0.4526	0.6177	UII	RS21
5771.0526	5771.0527	50218	0.0953	-0.1366	UI	P80
5776.8774	5776.8789	4127	0.5454	-1.5266	UII	RS21

continued ...

Observed Wavelength Å	Ritz Wavelength Å	Relative Flux ADU	Uncertainty mÅ	Offset from Ritz wavelength mÅ	Species	Source
5777.2916	5777.2897	3962	0.5718	1.9059	UI	P80
5780.5898	5780.5892	157036	0.0516	0.6699	UI	P80
5781.9452	5781.9447	27112	0.1344	0.4991	UI	P80
5782.8041	5782.8057	34268	0.1234	-1.5823	UI	P80
5783.6309	5783.6297	3337	0.9065	1.2246	UI	RS21
5787.2514	5787.2472	3667	0.5114	4.2396	UI	P80
5787.5930	5787.5914	16116	0.1722	1.5871	UI	P80
5791.7473	5791.7466	3912	0.6344	0.7027	UII	P80
5792.0107	5792.0114	7280	0.3106	-0.6481	UI	P80
5793.7868	5793.7874	3188	0.5448	-0.5985	UI	P80
5796.5187	5796.5195	20026	0.1550	-0.7614	UI	P80
5798.5287	5798.5282	15939	0.1725	0.4879	UII	P80
5799.3525	5799.3501	3073	0.5513	2.3471	UI	P80
5800.7761	5800.7763	11395	0.2185	-0.1928	UI	RS21
5802.1005	5802.1059	39096	0.1096	-5.3974	UI	P80
5803.6022	5803.6078	3440	0.5950	-5.5612	UII	RS21
5805.1945	5805.1934	29666	0.1229	1.0504	UI	P80
5808.6482	5808.6468	3342	0.6075	1.4449	UI	P80
5809.3043	5809.3087	9769	0.2493	-4.3919	UI	P80
5809.5643	5809.5658	3799	0.5181	-1.5865	UI	P80
5811.2640	5811.2662	4463	0.3933	-2.2208	UII	RS21
5811.7037	5811.7050	3201	0.5865	-1.2895	UI	P80
5812.0992	5812.1043	3901	0.6872	-5.0723	UII	RS21
5813.8190	5813.8214	44048	0.1052	-2.3257	UI	P80
5814.4155	5814.4171	51429	0.0969	-1.5349	UI	P80
5816.7636	5816.7621	15031	0.2172	1.5090	UII	P80
5817.9092	5817.9099	21280	0.1744	-0.6523	UI	P80
5819.0081	5819.0038	17944	0.2002	4.2732	UII	P80
5820.6119	5820.6131	11275	0.2487	-1.2213	UI	P80

continued ...

Observed Wavelength Å	Ritz Wavelength Å	Relative Flux ADU	Uncertainty mÅ	Offset from Ritz wavelength mÅ	Species	Source
5821.0285	5821.0282	4792	0.5294	0.3774	UI	P80
5821.8728	5821.8730	10585	0.3073	-0.1377	UI	P80
5823.8835	5823.8841	3526	0.7400	-0.5647	UI	P80
5825.3544	5825.3555	5465	0.4612	-1.1284	UI	P80
5826.1605	5826.1638	15782	0.2090	-3.2764	UI	P80
5829.0214	5829.0208	12564	0.2291	0.6402	UI	P80
5831.8119	5831.8154	27186	0.1428	-3.5252	UI	P80
5833.3180	5833.3161	2969	0.6857	1.8217	UI	P80
5833.6194	5833.6200	10495	0.2631	-0.6208	UI	P80
5835.1628	5835.1689	4531	0.5262	-6.0727	UII	P80
5835.4880	5835.4915	3180	0.6710	-3.5177	UI	P80
5836.0226	5836.0218	34057	0.1153	0.8037	UI	P80
5837.6830	5837.6838	15944	0.1912	-0.8225	UII	P80
5840.4866	5840.4874	6890	0.3147	-0.7722	UI	P80
5841.8174	5841.8159	3273	0.5474	1.4484	UI	RS21
5843.2838	5843.2891	5400	0.4180	-5.3120	UII	P80
5845.2484	5845.2489	12695	0.1991	-0.5092	UII	P80
5846.2074	5846.2063	8967	0.2754	1.1296	UII	P80
5849.1603	5849.1625	9621	0.2507	-2.1793	UI	P80
5852.0028	5852.0033	45098	0.0993	-0.4591	UI	P80
5853.9031	5853.9027	9700	0.2316	0.4340	UII	P80
5856.4462	5856.4465	27372	0.1304	-0.3567	UI	P80
5857.5717	5857.5698	2842	0.7562	1.9409	UI	P80
5859.6789	5859.6848	6254	0.3650	-5.8280	UI	P80
5862.0050	5862.0040	20232	0.1599	0.9273	UI	P80
5863.7177	5863.7138	3576	0.5626	3.9252	UI	P80
5866.2578	5866.2594	4704	0.4278	-1.6000	UI	P80
5868.0409	5868.0396	5961	0.4144	1.3106	UI	P80
5869.7361	5869.7367	7668	0.3551	-0.6347	UI	P80

continued ...

Observed Wavelength Å	Ritz Wavelength Å	Relative Flux ADU	Uncertainty mÅ	Offset from Ritz wavelength mÅ	Species	Source
5870.9271	5870.9284	18951	0.1809	-1.2749	UII	P80
5875.4107	5875.4099	7284	0.3734	0.8393	UI	P80
5877.7841	5877.7902	4603	0.6140	-6.0395	UI	RS21
5884.3967	5884.3967	8732	0.3241	0.0048	UI	P80
5886.9372	5886.9387	6136	0.4376	-1.5053	UII	RS21
5887.6243	5887.6254	4479	0.6184	-1.0053	UI	P80
5888.1133	5888.1143	4091	0.6660	-1.0251	UI	RS21
5888.5897	5888.5939	85851	0.0768	-4.2644	UII	RS21
5889.1539	5889.1509	5168	0.5863	3.0092	UI	RS21
5891.3573	5891.3592	6256	0.3329	-1.9196	UI	P80
5892.6224	5892.6208	51021	0.0938	1.6062	UI	P80
5893.6563	5893.6568	6605	0.3946	-0.4818	UII	P80
5898.7727	5898.7733	34665	0.1134	-0.5381	UI	P80
5900.2226	5900.2243	2738	0.6175	-1.6677	UI	P80
5901.8978	5901.9013	6955	0.3148	-3.4684	UI	P80
5902.4894	5902.4893	49455	0.1040	0.0950	UI	P80
5905.1230	5905.1219	6514	0.3213	1.1416	UI	P80
5907.7502	5907.7534	3039	0.5709	-3.2329	UI	P80
5910.3519	5910.3566	6022	0.4043	-4.6413	UI	P80
5911.5480	5911.5498	18423	0.1666	-1.7920	UI	P80
5914.6062	5914.6087	8127	0.3311	-2.4783	UI	P80
5919.6674	5919.6664	9931	0.2453	1.0273	UI	P80
5926.5028	5926.5027	4757	0.6942	0.1605	UII	RS21
5927.8714	5927.8713	4646	0.7146	0.1613	UI	P80
5928.8179	5928.8168	68573	0.0951	1.1620	UI	RS21
5929.3169	5929.3174	51155	0.0997	-0.5227	UI	P80
5932.4273	5932.4271	6810	0.4534	0.2202	UII	RS21
5933.8169	5933.8170	228015	0.0432	-0.1142	UI	P80
5934.4494	5934.4478	6412	0.4478	1.5091	UI	P80

continued ...

Observed Wavelength Å	Ritz Wavelength Å	Relative Flux ADU	Uncertainty mÅ	Offset from Ritz wavelength mÅ	Species	Source
5935.2455	5935.2454	7703	0.9389	0.1333	UII	RS21
5935.5026	5935.5069	13533	0.4711	-4.3370	UI	P80
5937.3718	5937.3735	7164	0.3652	-1.6936	UI	P80
5939.9920	5939.9897	18245	0.1838	2.2782	UI	P80
5940.6634	5940.6639	5443	0.5078	-0.5484	UI	P80
5942.0172	5942.0211	6083	0.4815	-3.9708	UI	RS21
5942.7513	5942.7490	50168	0.1260	2.3214	UI	RS21
5943.4080	5943.4114	14110	0.2282	-3.3762	UI	P80
5947.6699	5947.6712	15255	0.1841	-1.2855	UI	P80
5948.1764	5948.1709	4635	0.4451	5.5455	UI	P80
5948.5640	5948.5663	29583	0.1273	-2.2423	UI	P80
5949.6582	5949.6615	20767	0.1586	-3.2701	UI	P80
5952.0303	5952.0332	5272	0.5584	-2.8355	UII	P80
5954.3680	5954.3673	3015	0.6091	0.7915	UII	P80
5954.8986	5954.8986	7428	0.3018	-0.0090	UI	P80
5956.8566	5956.8591	45176	0.1028	-2.5060	UI	P80
5967.1510	5967.1501	3024	0.6334	0.8504	UI	P80
5968.7696	5968.7714	15718	0.1922	-1.8502	UI	P80
5971.4993	5971.5004	443365	0.0319	-1.0851	UI	P80
5972.7596	5972.7630	5958	0.4775	-3.3874	UII	P80
5974.7625	5974.7618	19973	0.1801	0.6154	UI	P80
5978.6891	5978.6895	10756	0.2293	-0.3936	UI	P80
5982.8695	5982.8685	21907	0.2051	1.0377	UI	P80
5983.7607	5983.7603	5895	0.5942	0.4874	UII	P80
5985.5684	5985.5719	14354	0.2427	-3.5009	UI	P80
5986.0988	5986.1004	349061	0.0361	-1.5922	UI	P80
5993.7472	5993.7479	4848	0.5988	-0.6739	UI	P80
5996.7514	5996.7527	21725	0.1806	-1.3184	UI	P80
5997.3093	5997.3106	225763	0.0429	-1.2986	UI	P80

continued ...

Observed Wavelength Å	Ritz Wavelength Å	Relative Flux ADU	Uncertainty mÅ	Offset from Ritz wavelength mÅ	Species	Source
5997.9576	5997.9592	94543	0.0697	-1.6411	UI	P80
5999.4066	5999.4082	106400	0.0653	-1.5636	UI	P80
6000.1759	6000.1775	20162	0.1748	-1.6835	UI	P80
6001.0768	6001.0759	6180	0.4917	0.9724	UII	P80
6003.7322	6003.7387	21005	0.1863	-6.4587	UI	P80
6004.8147	6004.8135	5593	0.5279	1.2443	UII	P80
6008.8358	6008.8358	8940	0.3473	-0.0555	UI	P80
6010.8602	6010.8603	13459	0.2076	-0.0705	UII	P80
6013.2614	6013.2605	10761	0.2432	0.8759	UI	P80
6014.0526	6014.0532	6399	0.3572	-0.5941	UI	P80
6016.7402	6016.7438	25621	0.1456	-3.6051	UI	P80
6017.5639	6017.5630	27905	0.1461	0.9798	UI	P80
6019.1905	6019.1905	32267	0.1215	-0.0205	UI	P80
6024.7235	6024.7224	3647	0.5383	1.0995	UI	P80
6028.1215	6028.1232	57612	0.0900	-1.6264	UI	P80
6028.6213	6028.6266	7876	0.3012	-5.3000	UI	P80
6031.1932	6031.1952	7769	0.3168	-1.9922	UI	P80
6034.5872	6034.5869	7294	0.3165	0.2108	UI	P80
6035.5471	6035.5483	19733	0.1610	-1.1842	UI	P80
6036.3118	6036.3120	3458	0.5697	-0.1708	UI	P80
6039.6169	6039.6169	36922	0.1065	0.0262	UI	P80
6039.9381	6039.9376	4612	0.6361	0.5070	UI	P80
6040.1222	6040.1236	5317	0.5876	-1.4271	UI	P80
6042.6600	6042.6600	6252	0.4792	0.0041	UI	P80
6045.0182	6045.0150	13851	0.2479	3.1816	UI	P80
6045.8484	6045.8547	5156	0.5687	-6.3178	UI	RS21
6046.4527	6046.4582	4982	0.7211	-5.4438	UI	P80
6048.3434	6048.3408	4295	0.6718	2.5779	UI	P80
6050.4870	6050.4850	84164	0.0864	1.9724	UI	P80

continued ...

Observed Wavelength Å	Ritz Wavelength Å	Relative Flux ADU	Uncertainty mÅ	Offset from Ritz wavelength mÅ	Species	Source
6050.6704	6050.6745	53517	0.1119	-4.0783	UI	P80
6051.7404	6051.7404	44505	0.1085	-0.0870	UI	P80
6056.8099	6056.8098	224446	0.0443	0.1203	UI	P80
6057.0799	6057.0814	67647	0.0892	-1.5144	UI	P80
6057.5329	6057.5359	4961	0.5894	-2.9368	UI	P80
6059.3728	6059.3724	78223	0.0801	0.4219	UI	RS21
6059.7412	6059.7454	11273	0.2834	-4.1617	UI	P80
6060.1790	6060.1809	3849	0.6537	-1.9153	UI	P80
6060.4883	6060.4901	12962	0.2313	-1.8621	UI	P80
6062.3054	6062.3090	127372	0.0604	-3.6388	UI	P80
6067.2205	6067.2220	15939	0.1840	-1.5332	UI	P80
6070.1806	6070.1865	3096	0.6627	-5.8682	UI	P80
6072.7034	6072.7057	8247	0.2808	-2.2812	UI	P80
6074.8637	6074.8642	13464	0.2131	-0.5715	UI	P80
6076.1886	6076.1890	6310	0.3440	-0.3743	UI	P80
6077.2898	6077.2906	296110	0.0381	-0.8308	UI	P80
6078.1132	6078.1133	3731	0.4709	-0.0996	UI	P80
6080.3799	6080.3783	13022	0.2067	1.5763	UI	P80
6085.7598	6085.7569	5170	0.4746	2.9035	UI	P80
6087.3390	6087.3369	6457	0.3224	2.1130	UI	P80
6087.5412	6087.5432	4423	0.4928	-2.0004	UI	P80
6088.1066	6088.1066	3196	0.5268	-0.0052	UI	P80
6089.1864	6089.1901	24048	0.6340	-3.7133	UI	P80
6091.2799	6091.2828	7780	0.2878	-2.9106	UI	P80
6101.4789	6101.4817	8971	0.3361	-2.8047	UI	P80
6101.7785	6101.7784	78820	0.0808	0.0408	UI	P80
6107.7391	6107.7427	14584	0.2222	-3.5524	UI	P80
6110.3093	6110.3081	3798	0.8163	1.2069	UI	P80
6110.6846	6110.6848	10789	0.3122	-0.2224	UI	P80

continued ...

Observed Wavelength Å	Ritz Wavelength Å	Relative Flux ADU	Uncertainty mÅ	Offset from Ritz wavelength mÅ	Species	Source
6114.2765	6114.2743	8029	0.3471	2.1268	UI	P80
6114.9230	6114.9200	581711	0.0283	2.9539	UI	RS21
6116.1587	6116.1644	6784	0.3962	-5.6836	UI	P80
6116.6672	6116.6639	4444	0.5663	3.2117	UI	P80
6118.2036	6118.1975	3566	0.7179	6.1209	UI	RS21
6120.6434	6120.6454	25175	0.1488	-2.0357	UI	P80
6121.4357	6121.4363	15531	0.2016	-0.6439	UI	P80
6125.0186	6125.0216	4780	0.4830	-3.0305	UII	P80
6127.2260	6127.2198	4701	0.5881	6.1945	UI	P80
6129.7209	6129.7230	139350	0.0552	-2.1228	UI	P80
6130.2007	6130.2009	7495	0.3076	-0.1749	UI	P80
6132.6172	6132.6188	35745	0.1210	-1.6340	UI	P80
6135.7222	6135.7199	5032	0.4007	2.2062	UI	P80
6140.3746	6140.3778	8444	0.2761	-3.1714	UI	P80
6142.3291	6142.3323	12100	0.2191	-3.1291	UI	P80
6143.6432	6143.6438	2715	0.6478	-0.6423	UII	P80
6147.9274	6147.9297	8327	0.2712	-2.2159	UI	P80
6150.0800	6150.0811	3123	0.5694	-1.1470	UII	P80
6152.2598	6152.2599	37008	0.1173	-0.1635	UI	P80
6153.6708	6153.6704	23518	0.1494	0.3808	UI	RS21
6154.3683	6154.3719	3701	0.5970	-3.5889	UI	P80
6159.3921	6159.3923	3794	0.5040	-0.1440	UI	P80
6161.9687	6161.9705	7403	0.3651	-1.7996	UI	P80
6164.2423	6164.2450	9954	0.3533	-2.6410	UII	RS21
6164.5121	6164.5145	60976	0.0958	-2.4160	UI	P80
6165.8196	6165.8221	35751	0.1299	-2.5900	UI	P80
6167.6019	6167.6023	12279	0.2667	-0.3399	UI	P80
6169.4925	6169.4920	22532	0.1700	0.5654	UI	P80
6171.8612	6171.8587	261266	0.0439	2.4453	UI	P80

continued ...

Observed Wavelength Å	Ritz Wavelength Å	Relative Flux ADU	Uncertainty mÅ	Offset from Ritz wavelength mÅ	Species	Source
6172.6080	6172.6052	11674	0.3533	2.7111	UI	P80
6173.8982	6173.8948	4058	0.7166	3.4566	UII	RS21
6174.3775	6174.3800	73983	0.0856	-2.4364	UI	P80
6174.8883	6174.8876	22641	0.1725	0.7373	UI	P80
6175.3927	6175.3949	332121	0.0367	-2.1794	UI	P80
6176.4702	6176.4709	23572	0.1599	-0.7576	UI	P80
6181.3836	6181.3805	8235	0.3505	3.1882	UI	P80
6181.6949	6181.6936	5274	0.5551	1.2866	UI	P80
6182.8068	6182.8099	6589	0.4261	-3.1611	UI	P80
6183.1118	6183.1147	11619	0.2804	-2.8487	UI	P80
6184.2822	6184.2864	5252	0.5117	-4.2294	UI	P80
6184.9808	6184.9862	3334	0.7967	-5.4875	UII	RS21
6188.0791	6188.0789	4319	0.6827	0.1927	UI	P80
6194.6245	6194.6247	5695	0.3740	-0.1576	UI	P80
6196.5236	6196.5257	13580	0.2136	-2.0759	UI	P80
6197.9821	6197.9798	3045	0.6117	2.2137	UI	P80
6198.3995	6198.3994	13132	0.2175	0.1014	UI	P80
6201.9736	6201.9744	16414	0.1850	-0.8101	UI	P80
6203.3690	6203.3713	18628	0.1786	-2.2797	UI	P80
6205.7610	6205.7649	4692	0.4238	-3.8359	UI	P80
6206.8537	6206.8564	3593	0.5484	-2.6680	UI	P80
6211.2026	6211.2000	2969	0.7661	2.6202	UI	P80
6214.3386	6214.3412	4212	0.4779	-2.6181	UI	P80
6215.3728	6215.3738	101867	0.0680	-1.0188	UI	P80
6216.8601	6216.8591	14988	0.1835	0.9800	UI	P80
6220.2886	6220.2895	8945	0.2817	-0.9236	UI	P80
6221.5766	6221.5767	3907	0.5243	-0.1254	UII	P80
6222.1489	6222.1496	28745	0.1334	-0.6669	UI	P80
6223.9932	6223.9870	10696	0.3455	6.2145	UI	P80

continued ...

Observed Wavelength Å	Ritz Wavelength Å	Relative Flux ADU	Uncertainty mÅ	Offset from Ritz wavelength mÅ	Species	Source
6226.8680	6226.8707	3810	0.6477	-2.6267	UII	RS21
6227.3453	6227.3392	7231	0.4191	6.0999	UI	P80
6227.9734	6227.9746	16925	0.2040	-1.1901	UI	P80
6229.6381	6229.6361	14465	0.2322	2.0175	UI	P80
6230.0709	6230.0740	5224	0.5318	-3.0158	UI	P80
6231.2188	6231.2196	10421	0.2889	-0.7915	UI	P80
6231.6393	6231.6402	9875	0.3074	-0.9855	UI	P80
6232.2847	6232.2867	7812	0.3876	-1.9959	UI	P80
6232.5336	6232.5333	6739	0.4330	0.2987	UII	RS21
6234.3022	6234.3036	147809	0.0599	-1.3567	UI	P80
6238.1940	6238.1957	26224	0.1486	-1.6389	UI	P80
6239.4420	6239.4458	5940	0.4924	-3.8248	UI	P80
6239.9894	6239.9893	4084	0.7352	0.1460	UI	P80
6244.0431	6244.0469	3917	0.6205	-3.8699	UI	P80
6246.5327	6246.5341	90942	0.0734	-1.4382	UI	P80
6251.7984	6251.8015	55049	0.0973	-3.1382	UI	P80
6252.6448	6252.6443	4897	0.5006	0.5275	UI	P80
6253.6461	6253.6473	6498	0.3719	-1.2059	UI	P80
6253.8731	6253.8723	4427	0.5920	0.7932	UI	P80
6255.1093	6255.1104	3086	0.5771	-1.0974	UI	P80
6256.7146	6256.7138	4066	0.4956	0.8087	UI	P80
6258.9970	6259.0018	2751	0.8907	-4.7864	UI	RS21
6263.9302	6263.9315	9672	0.2700	-1.2574	UI	P80
6268.6715	6268.6705	23780	0.1448	1.0050	UI	P80
6270.5624	6270.5624	28768	0.1369	0.0753	UI	P80
6272.5470	6272.5414	2915	0.5805	5.5867	UI	P80
6274.1071	6274.1130	2613	0.7037	-5.9142	UI	P80
6280.1814	6280.1825	11223	0.2391	-1.1258	UII	P80
6282.2117	6282.2120	4311	0.5201	-0.2856	UI	RS21

continued ...

Observed Wavelength Å	Ritz Wavelength Å	Relative Flux ADU	Uncertainty mÅ	Offset from Ritz wavelength mÅ	Species	Source
6282.5662	6282.5640	6008	0.4048	2.1893	UI	P80
6283.8796	6283.8814	3031	0.6730	-1.7503	UI	P80
6284.5766	6284.5757	17065	0.1838	0.8489	UI	P80
6285.4336	6285.4355	3474	0.6547	-1.8919	UII	RS21
6288.4116	6288.4142	5847	0.4824	-2.5914	UI	P80
6289.0756	6289.0787	4374	0.7429	-3.0535	UI	P80
6291.4510	6291.4480	9762	0.3664	2.9715	UII	P80
6292.0224	6292.0211	121912	0.0679	1.3658	UII	P80
6293.3267	6293.3277	479352	0.0321	-1.0288	UII	P80
6293.9743	6293.9716	28191	0.1650	2.7154	UI	P80
6295.8754	6295.8737	5566	0.5290	1.7434	UI	P80
6298.5314	6298.5326	224500	0.0456	-1.1779	UI	P80
6299.2435	6299.2453	6700	0.4619	-1.7511	UI	P80
6302.8396	6302.8433	5198	0.6792	-3.6123	UII	RS21
6303.5685	6303.5725	4244	0.7598	-4.0101	UI	P80
6306.9641	6306.9582	28722	0.1500	5.9422	UI	P80
6308.7240	6308.7259	4840	0.6075	-1.8540	UI	RS21
6311.6768	6311.6824	4641	0.7152	-5.6253	UI	P80
6312.6856	6312.6885	3486	0.7990	-2.8861	UI	RS21
6318.3293	6318.3267	11785	0.2599	2.5856	UII	P80
6318.6149	6318.6168	4795	0.5835	-1.9796	UI	P80
6319.4750	6319.4796	3296	0.6594	-4.6858	UI	P80
6321.2579	6321.2579	8173	0.3041	-0.0039	UI	P80
6322.3625	6322.3627	6390	0.3558	-0.1426	UII	P80
6323.3776	6323.3757	4737	0.5082	1.8939	UI	P80
6324.1113	6324.1078	3980	0.5850	3.5020	UI	P80
6324.4399	6324.4363	22838	0.1807	3.5141	UI	P80
6327.3890	6327.3892	10339	0.2888	-0.2789	UI	P80
6327.9713	6327.9720	4416	0.4793	-0.7462	UI	P80

continued ...

Observed Wavelength Å	Ritz Wavelength Å	Relative Flux ADU	Uncertainty mÅ	Offset from Ritz wavelength mÅ	Species	Source
6330.7542	6330.7548	4754	0.4460	-0.5774	UII	P80
6331.6519	6331.6526	3869	0.5105	-0.6867	UI	P80
6332.2578	6332.2593	6206	0.3657	-1.5123	UI	P80
6338.7349	6338.7338	18584	0.2006	1.0797	UI	P80
6343.7078	6343.7114	2689	0.6382	-3.5845	UI	P80
6348.2315	6348.2259	6019	0.4662	5.6086	UI	RS21
6350.0280	6350.0298	6609	0.3352	-1.7505	UI	P80
6351.0370	6351.0383	3559	0.5076	-1.3376	UI	P80
6353.4159	6353.4135	18692	0.1971	2.4258	UI	P80
6354.8926	6354.8925	12662	0.2429	0.0533	UI	P80
6355.5299	6355.5246	8206	0.3547	5.3042	UI	P80
6358.5820	6358.5848	4100	0.6953	-2.7520	UI	P80
6359.2889	6359.2898	559569	0.0291	-0.9349	UI	P80
6359.6176	6359.6237	14134	0.2721	-6.0801	UI	P80
6360.7272	6360.7281	21953	0.1826	-0.9048	UI	P80
6362.3814	6362.3837	3623	0.9236	-2.3015	UII	RS21
6364.1500	6364.1446	13406	0.2469	5.3735	UI	P80
6364.4736	6364.4711	9024	0.3336	2.5727	UI	P80
6367.6576	6367.6559	18995	0.1884	1.6657	UI	P80
6369.1077	6369.1142	7960	0.4281	-6.5595	UI	P80
6369.8527	6369.8521	78448	0.0825	0.5639	UI	P80
6371.7005	6371.7017	5079	0.6136	-1.1532	UI	P80
6372.4506	6372.4509	717177	0.0247	-0.2921	UI	P80
6372.9910	6372.9904	76452	0.0841	0.5949	UI	P80
6374.1472	6374.1495	29125	0.1424	-2.2866	UI	P80
6374.4754	6374.4738	11327	0.2889	1.6479	UI	P80
6374.7222	6374.7211	6637	0.4752	1.1403	UII	RS21
6375.9668	6375.9694	10115	0.2923	-2.5893	UII	RS21
6376.7205	6376.7176	4234	0.6454	2.9187	UI	P80

continued ...

Observed Wavelength Å	Ritz Wavelength Å	Relative Flux ADU	Uncertainty mÅ	Offset from Ritz wavelength mÅ	Species	Source
6379.6207	6379.6178	12904	0.2763	2.9705	UII	P80
6380.4470	6380.4508	6498	0.4552	-3.8348	UI	P80
6383.5702	6383.5717	99901	0.0713	-1.4661	UI	P80
6384.7185	6384.7195	100177	0.0776	-1.0143	UI	RS21
6386.8374	6386.8374	3519	0.5950	-0.0537	UII	RS21
6388.6061	6388.6035	6417	0.4254	2.5618	UI	P80
6389.7871	6389.7895	120467	0.0630	-2.3670	UI	P80
6392.7603	6392.7622	294055	0.0411	-1.8765	UI	P80
6397.1615	6397.1561	67227	0.0931	5.3585	UI	P80
6404.4588	6404.4580	17827	0.1798	0.7425	UI	P80
6407.1390	6407.1344	2564	0.7399	4.5640	UI	P80
6409.8572	6409.8568	12428	0.2251	0.3583	UI	P80
6411.5928	6411.5943	33654	0.1290	-1.5516	UI	P80
6416.3065	6416.3093	294281	0.0420	-2.8436	UI	RS21
6416.8723	6416.8756	2966	0.7317	-3.3624	UI	P80
6417.6627	6417.6681	4994	0.5413	-5.3909	UI	P80
6418.3721	6418.3706	12287	0.3067	1.4759	UI	RS21
6420.5004	6420.5054	3271	0.8024	-4.9182	UI	P80
6421.4163	6421.4168	3594	0.7125	-0.4763	UI	P80
6422.2233	6422.2273	3953	0.7216	-4.0390	UI	P80
6424.8725	6424.8698	9485	0.3319	2.7240	UII	P80
6425.4492	6425.4480	3446	0.8497	1.1488	UII	P80
6427.5008	6427.4979	29740	0.1522	2.8859	UII	P80
6428.6893	6428.6922	48860	0.1168	-2.8996	UI	P80
6430.9366	6430.9376	81939	0.0818	-1.0322	UI	P80
6434.6306	6434.6290	8711	0.4527	1.5608	UI	P80
6435.1209	6435.1273	5946	0.4933	-6.4524	UI	RS21
6441.3419	6441.3455	8168	0.3393	-3.6088	UI	P80
6442.5559	6442.5564	23576	0.1613	-0.4449	UI	P80

continued ...

Observed Wavelength Å	Ritz Wavelength Å	Relative Flux ADU	Uncertainty mÅ	Offset from Ritz wavelength mÅ	Species	Source
6443.8631	6443.8655	15712	0.2506	-2.3573	UI	RS21
6445.8085	6445.8114	5584	0.4377	-2.8455	UI	P80
6448.0200	6448.0253	4951	0.5319	-5.3272	UII	P80
6448.5784	6448.5797	18180	0.2061	-1.2901	UII	P80
6449.9106	6449.9067	6263	0.5217	3.8793	UI	P80
6451.2022	6451.1988	5774	0.4735	3.3759	UI	P80
6458.9581	6458.9637	2841	0.6753	-5.6236	UI	P80
6460.3497	6460.3439	4394	0.4485	5.8128	UI	P80
6461.9327	6461.9327	14022	0.2143	0.0738	UI	P80
6464.9888	6464.9847	171623	0.0551	4.0524	UI	P80
6466.5786	6466.5803	13633	0.2737	-1.6563	UI	RS21
6467.0407	6467.0378	3240	0.5626	2.8485	UI	P80
6479.9576	6479.9563	13271	0.2490	1.3269	UII	P80
6481.7281	6481.7283	34225	0.1315	-0.1653	UI	P80
6486.6423	6486.6449	15182	0.2306	-2.5727	UI	P80
6487.0329	6487.0366	30346	0.1465	-3.7078	UI	P80
6491.3287	6491.3306	5840	0.5177	-1.9563	UI	P80
6496.8011	6496.8056	14617	0.2444	-4.4778	UI	P80
6498.8003	6498.7944	6699	0.4811	5.9701	UI	P80
6499.7340	6499.7310	4415	0.5914	2.9588	UI	P80
6503.6188	6503.6216	260248	0.0473	-2.7868	UI	P80
6506.2813	6506.2827	7835	0.4070	-1.4783	UI	P80
6506.7969	6506.7935	4199	0.5808	3.4259	UI	RS21
6507.3756	6507.3750	6132	0.4148	0.5595	UI	P80
6507.6712	6507.6666	3918	0.7413	4.6124	UII	P80
6508.1738	6508.1780	7091	0.5443	-4.1759	UII	RS21
6510.7810	6510.7857	4115	0.6198	-4.6851	UI	RS21
6511.1516	6511.1497	3657	0.7300	1.8754	UII	RS21
6515.4171	6515.4160	5635	0.4442	1.0900	UI	P80

continued ...

Observed Wavelength Å	Ritz Wavelength Å	Relative Flux ADU	Uncertainty mÅ	Offset from Ritz wavelength mÅ	Species	Source
6515.9600	6515.9601	3190	0.6620	-0.0779	UI	P80
6517.6663	6517.6659	8725	0.3506	0.3912	UI	P80
6518.9468	6518.9472	134077	0.0618	-0.3495	UI	P80
6519.4927	6519.4939	3384	0.7398	-1.2717	UI	P80
6520.9829	6520.9815	25076	0.1522	1.4261	UI	P80
6521.9917	6521.9902	8007	0.3080	1.4391	UI	P80
6523.1618	6523.1626	4252	0.4337	-0.7895	UI	P80
6524.4536	6524.4543	2688	0.6377	-0.6759	UI	P80
6526.0793	6526.0773	19238	0.1788	2.0356	UI	P80
6527.0475	6527.0459	24270	0.1639	1.5858	UI	P80
6531.7047	6531.7085	3496	0.5650	-3.8810	UI	P80
6534.3583	6534.3552	7335	0.3319	3.1248	UI	P80
6542.9892	6542.9848	35589	0.1245	4.4088	UI	P80
6544.4919	6544.4911	5828	0.3614	0.7727	UI	P80
6545.7387	6545.7331	10624	0.2712	5.5923	UI	P80
6549.8867	6549.8843	3577	0.5567	2.3499	UI	RS21
6550.7639	6550.7620	2719	0.6536	1.9470	UI	P80
6551.8178	6551.8177	7784	0.3071	0.1888	UI	P80
6552.7585	6552.7575	18167	0.1847	1.0214	UI	P80
6555.0099	6555.0103	243733	0.0477	-0.3973	UI	P80
6555.8970	6555.8968	9622	0.3151	0.1331	UI	P80
6556.8620	6556.8630	14061	0.2326	-1.0852	UI	P80
6558.9375	6558.9329	4748	0.5321	4.6235	UI	P80
6564.1615	6564.1660	4177	0.7076	-4.4981	UI	P80
6566.2147	6566.2139	3584	0.6609	0.7721	UI	RS21
6566.8103	6566.8116	11211	0.2683	-1.2546	UI	P80
6573.0228	6573.0236	2991	0.7910	-0.8588	UI	RS21
6573.8191	6573.8172	4042	0.6029	1.9386	UI	P80
6574.7400	6574.7435	7511	0.3479	-3.4367	UI	P80

continued ...

Observed Wavelength Å	Ritz Wavelength Å	Relative Flux ADU	Uncertainty mÅ	Offset from Ritz wavelength mÅ	Species	Source
6578.7955	6578.7959	19781	0.1767	-0.3460	UI	P80
6579.5200	6579.5172	6779	0.4436	2.7720	UI	P80
6580.6379	6580.6380	3162	0.6953	-0.1483	UI	P80
6582.2301	6582.2340	3880	0.5413	-3.9354	UII	P80
6582.7759	6582.7779	30785	0.1419	-1.9969	UI	P80
6585.2093	6585.2090	33863	0.1294	0.3748	UI	P80
6586.8973	6586.9004	4017	0.5560	-3.1398	UI	P80
6587.8410	6587.8406	5254	0.4338	0.4169	UII	P80
6588.9039	6588.8998	4652	0.5529	4.1417	UI	P80
6590.0542	6590.0569	7469	0.3466	-2.6559	UII	P80
6601.3905	6601.3906	13644	0.2326	-0.1087	UI	P80
6603.3393	6603.3412	4051	0.5037	-1.9020	UII	P80
6603.9902	6603.9921	35120	0.1258	-1.9062	UI	P80
6607.3289	6607.3292	4578	0.5009	-0.3002	UII	P80
6609.2372	6609.2351	2392	0.6668	2.0497	UI	P80
6616.7507	6616.7511	3284	0.5318	-0.3807	UI	P80
6619.2681	6619.2659	3137	0.6028	2.2287	UI	P80
6620.5285	6620.5317	219184	0.0473	-3.2012	UI	P80
6621.7741	6621.7779	10616	0.2491	-3.8511	UII	P80
6622.8407	6622.8348	3303	0.5814	5.9609	UII	P80
6625.2933	6625.2955	58187	0.1013	-2.1512	UI	P80
6629.0456	6629.0455	24081	0.1753	0.0733	UI	P80
6629.8532	6629.8583	3396	0.6806	-5.0223	UI	P80
6630.1790	6630.1820	13808	0.2366	-3.0599	UI	P80
6633.4150	6633.4132	9579	0.3150	1.7963	UI	P80
6641.0745	6641.0747	10053	0.3180	-0.2483	UI	P80
6642.3445	6642.3438	6028	0.4221	0.7665	UI	P80
6647.7928	6647.7933	51451	0.1057	-0.5203	UI	P80
6649.5419	6649.5404	2998	0.7752	1.4352	UI	P80

continued ...

Observed Wavelength Å	Ritz Wavelength Å	Relative Flux ADU	Uncertainty mÅ	Offset from Ritz wavelength mÅ	Species	Source
6650.4798	6650.4800	3079	0.7747	-0.1509	UI	P80
6653.3571	6653.3578	2970	0.7975	-0.6973	UI	P80
6656.8169	6656.8185	113542	0.0843	-1.6453	UI	P80
6657.6921	6657.6961	26428	0.1614	-3.9982	UI	P80
6662.5413	6662.5434	5486	0.4615	-2.1125	UI	P80
6672.6652	6672.6667	12275	0.2240	-1.4771	UI	P80
6677.2799	6677.2845	329990	0.0421	-4.5839	UI	RS21
6683.3839	6683.3845	80180	0.0815	-0.6336	UI	P80
6685.9266	6685.9276	3773	0.5098	-0.9784	UI	P80
6688.3971	6688.4022	4247	0.5125	-5.0543	UI	P80
6691.2028	6691.1983	13521	0.2303	4.4788	UI	P80
6692.0249	6692.0224	10198	0.2649	2.5040	UI	P80
6694.2363	6694.2406	5975	0.3911	-4.2869	UI	P80
6697.7129	6697.7151	5242	0.4637	-2.1636	UI	P80
6701.5227	6701.5182	12673	0.2800	4.4563	UI	P80
6707.5980	6707.5949	4195	0.6056	3.1449	UI	RS21
6711.1240	6711.1255	4843	0.5200	-1.4787	UI	P80
6716.6466	6716.6476	14167	0.2332	-1.0145	UI	P80
6717.4493	6717.4502	9012	0.3190	-0.8316	UI	P80
6717.9622	6717.9633	26904	0.1530	-1.0930	UI	P80
6719.2188	6719.2147	25269	0.1640	4.1895	UI	RS21
6719.9031	6719.9071	4967	0.6223	-4.0750	UI	P80
6721.5615	6721.5617	4297	0.5466	-0.2204	UI	P80
6730.4759	6730.4752	7428	0.3828	0.7993	UI	RS21
6732.1507	6732.1566	3698	0.5775	-5.8848	UI	P80
6733.1424	6733.1440	5639	0.4202	-1.6558	UI	P80
6735.0330	6735.0355	5052	0.6092	-2.5233	UI	P80
6736.8020	6736.8044	116343	0.0681	-2.4285	UI	P80
6738.1702	6738.1742	18882	0.1905	-3.9569	UI	RS21

continued ...

Observed Wavelength Å	Ritz Wavelength Å	Relative Flux ADU	Uncertainty mÅ	Offset from Ritz wavelength mÅ	Species	Source
6739.6160	6739.6137	7687	0.3399	2.2958	UII	P80
6741.3605	6741.3632	84705	0.0794	-2.6631	UI	P80
6743.1138	6743.1150	4256	0.4548	-1.1878	UI	P80
6748.2869	6748.2886	16577	0.1926	-1.7194	UI	P80
6751.6314	6751.6315	16534	0.2313	-0.0750	UI	P80
6752.8321	6752.8260	531180	0.0345	6.1674	UI	RS21
6754.9266	6754.9282	12828	0.2248	-1.6034	UI	P80
6767.2607	6767.2598	4918	0.4204	0.9081	UII	P80
6768.6436	6768.6406	23142	0.1646	3.0336	UI	P80
6770.6670	6770.6681	6569	0.4761	-1.1021	UI	P80
6771.0009	6771.0008	6595	0.4137	0.1352	UII	RS21
6772.0872	6772.0861	3876	0.7670	1.0868	UI	P80
6773.2371	6773.2376	9987	0.3006	-0.5062	UI	P80
6776.8860	6776.8861	4709	0.5089	-0.1368	UII	P80
6780.6325	6780.6315	32895	0.1424	0.9890	UI	P80
6788.7595	6788.7627	8623	0.3333	-3.1809	UI	P80
6790.3018	6790.3018	158174	0.0590	0.0177	UI	P80
6791.4273	6791.4240	3496	0.6701	3.3324	UI	P80
6792.3135	6792.3130	4239	0.5744	0.4438	UI	P80
6793.7618	6793.7609	4709	0.5035	0.8704	UI	P80
6796.4403	6796.4419	4499	0.5271	-1.5135	UII	RS21
6804.9422	6804.9453	4862	0.4926	-3.0683	UI	P80
6805.2115	6805.2109	3785	0.6519	0.6822	UI	P80
6812.9872	6812.9908	26566	0.1589	-3.5835	UI	P80
6816.1293	6816.1317	3997	0.5355	-2.3375	UI	P80
6818.2982	6818.3013	121562	0.0684	-3.0402	UI	P80
6819.2910	6819.2850	3121	0.5883	5.9408	UI	P80
6820.1265	6820.1269	3596	0.5332	-0.3679	UI	P80
6820.7653	6820.7653	161104	0.0578	-0.0040	UI	P80

continued ...

Observed Wavelength Å	Ritz Wavelength Å	Relative Flux ADU	Uncertainty mÅ	Offset from Ritz wavelength mÅ	Species	Source
6823.9371	6823.9398	10622	0.2626	-2.6351	UI	P80
6824.4556	6824.4575	26737	0.1662	-1.8994	UI	P80
6829.3295	6829.3307	9556	0.2744	-1.1632	UI	P80
6830.8513	6830.8495	5793	0.3844	1.7800	UI	P80
6832.7223	6832.7188	16291	0.2019	3.5403	UI	P80